

# Metals Processing Laboratory Users (MPLUS) Facility Annual Report FY 2001 (October 1, 2000-September 30, 2001)



## DOCUMENT AVAILABILITY

Reports produced after January 1, 1996, are generally available free via the U.S. Department of Energy (DOE) Information Bridge.

**Web site** <http://www.osti.gov/bridge>

Reports produced before January 1, 1996, may be purchased by members of the public from the following source:

National Technical Information Service  
5285 Port Royal Road  
Springfield, VA 22161  
**Telephone** 703-605-6000 (1-800-553-6847)  
**TDD** 703-487-4639  
**Fax** 703-605-6900  
**E-mail** [info@ntis.fedworld.gov](mailto:info@ntis.fedworld.gov)  
**Web site** <http://www.ntis.gov/support/ordernowabout.htm>

Reports are available to DOE employees, DOE contractors, Energy Technology Data Exchange (ETDE) representatives, and International Nuclear Information System (INIS) representatives from the following source:

Office of Scientific and Technical Information  
P.O. Box 62  
Oak Ridge, TN 37831  
**Telephone** 865-576-8401  
**Fax** 865-576-5728  
**E-mail** [reports@adonis.osti.gov](mailto:reports@adonis.osti.gov)  
**Web site** <http://www.osti.gov/contact.html>

This report was prepared as an account of work sponsored by an agency of the United States Government. Neither the United States Government nor any agency thereof, nor any of their employees, makes any warranty, express or implied, or assumes any legal liability or responsibility for the accuracy, completeness, or usefulness of any information, apparatus, product, or process disclosed, or represents that its use would not infringe privately owned rights. Reference herein to any specific commercial product, process, or service by trade name, trademark, manufacturer, or otherwise, does not necessarily constitute or imply its endorsement, recommendation, or favoring by the United States Government or any agency thereof. The views and opinions of authors expressed herein do not necessarily state or reflect those of the United States Government or any agency thereof.

**Metals Processing Laboratory Users (MPLUS) Facility**

**ANNUAL REPORT:  
OCTOBER 1, 2000, THROUGH SEPTEMBER 30, 2001**

Compiled by:  
P. Angelini  
M. L. Atchley

Published May 2003

Research sponsored by the  
U.S. Department of Energy,  
Office of Energy Efficiency and Renewable Energy,  
Industrial Technologies Program,  
Industrial Materials for the Future (IMF)  
and Industries of the Future (IOF) Activities  
1000 Independence Avenue NW  
Washington, DC 20585-0121

OAK RIDGE NATIONAL LABORATORY  
P.O. Box 2008  
Oak Ridge, Tennessee 37831-6285  
managed by  
UT-Battelle, LLC  
for the  
U.S. DEPARTMENT OF ENERGY  
under contract DE-AC05-00OR22725



## CONTENTS

---

INTRODUCTION.....	1
HIGHLIGHTS .....	3
Stress Analysis in Thin Surface Layers (Vista Engineering Inc.).....	7
Development of Infrared Thermal Processing Techniques for Improving the Wear and Corrosion Resistance of Coatings (Caterpillar Inc.) .....	11
The Effect of Thermal Process Parameters on the Phase Transformation Behavior in Fully Austenitized, Medium-Carbon Alloy Steel (Ispat Inland, Inc.) .....	13
Recovery Boiler Wall Tube Temperature Measurements (Babcock & Wilcox) .....	15
Analyses of Weld Overlay Tubes (Babcock & Wilcox) .....	19
Investigation of Oxidation of Superalloys at High Pressures and Temperatures (GE Aircraft Engines) .....	23
Evaluation of Filler Metals for Improved Elevated Temperature Strength of Aluminum Welds (Eagle Racing).....	25
Pyrowear 53: Dilatometry to Determine Phase Transformation Kinetics (Deformation Control Technology) .....	29
Dilatometric Study of Phase Transformati and Resultant Phase Fractions in Forged 1550 Steel for Comparison to and Definition of the Microstructures of Induction-Hardened Parts (Cummins Engine Co.) .....	33
Detection of Fabrication Defects and Oxidation in Aluminum Recycled Scrap Ingots (RSI) (Logan Aluminum) .....	35
Dilatometric Characterization of the Influence of a Standard Heat-Treating Process (the T-6 Temper) On the Dimensional Stability of a Die Cast Aluminum Alloy (Ohio State University).....	39
Hardenability of Next-Generation High-Strength Steels for Oil/Natural Gas Transportation Pipelines (Emc <sup>2</sup> ).....	43
Statistical Analysis of Time-Series Data on Temperature and Resistivity Collected from Recovery Boiler Floor Tube Membranes (Mead Central Research)	45

Preparation of Spheres (1 to 2 mm diam) of a Magnesium Alloy for Improving Process Efficiency of Thixomolding® (Thixomat)	47
Feasibility Study for Hot Extrusion of High Toughness Cemented Carbide Composite (Smith International, Inc.)	49
Select Alloys, Conduct In-Plant Tests, and Characterize Test Coupons of Candidate Hood Materials (Weirton Steel Corporation)	51
The Effect of Boron and Zirconium on the Resistance of HAYNES® 214™ Alloy to Strain Age Cracking (Haynes International Inc.)	53
Detection of Plant Cell Dimensions in Loblolly Pine Wood using Micro-CAT Scan Techniques (Weyerhaeuser Company)	55
Determination of True Stress-Strain Curves of Steels at Elevated Temperatures (Caterpillar Inc.)	59
Forming of Thick Section Material using The Vortek Water Stabilized Plasma Lamp (Native American Technologies Company)	61
Residual Stress Determination in Friction Stir Welded 2024-T3 Aluminum (University of South Carolina)	65
Soldering/Brazing for Automotive Aluminum Panels using Arc Lamp as a Heating Method (Ford Motor Company)	69
Rapid Infrared Preheating of Extrusion Die	71
Fabrication, Heat-Treating Microstructures, and Tensile Testing of a High-strength 3Cr-3W-V(Ta) Alloy Plate (Nooter Consulting Services)	75
Improving the Surface Finishing of Extruded 6262 Alloy Billet (Alcoa Engineered Productx)	79
Energy Savings during the Extrusion of 6061 Alloy (Alcoa Engineered Products)	83
Simulation of Sulfur Segregation in Steels (Caterpillar Inc.)	87
Development of Seal Coatings for Ceramic Refractories for Molten Aluminum (Pyrotek)	89
Thermochemical Optimization of Float Glass Composition (Visteon Glass Systems)	93

Reactive-Gas Inert Anode Concept (MMPaCT, Inc.) .....	95
LIST OF PROJECTS .....	97
STAFF CONTACTS AND GENERAL INFORMATION .....	101
ACKNOWLEDGEMENT .....	103





## INTRODUCTION

---

### Metals Processing Laboratory Users Facility (MPLUS)

The Metals Processing Laboratory Users Facility (MPLUS) is a Department of Energy (DOE), Energy Efficiency and Renewable Energy, Industrial Technologies Program user facility designated to assist researchers in key industries, universities, and federal laboratories in improving energy efficiency, improving environmental aspects, and increasing competitiveness. The goal of MPLUS is to provide access to the specialized technical expertise and equipment needed to solve metals processing issues that limit the development and implementation of emerging metals processing technologies. The scope of work can also extend to other types of materials.

MPLUS has four primary User Centers including:

Processing – casting, powder metallurgy, deformation processing including (extrusion, forging, rolling), melting, thermomechanical processing, high density infrared processing

Joining - welding, monitoring and control, solidification, brazing, bonding,

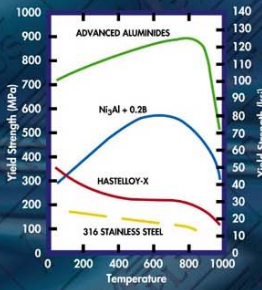
Characterization – corrosion, mechanical properties, fracture mechanics, microstructure, nondestructive examination, computer-controlled dilatometry, and emissivity.

Materials/Process Modeling – mathematical design and analyses, high performance computing, process modeling, solidification/deformation, microstructure evolution, thermodynamic and kinetic, and materials data bases.

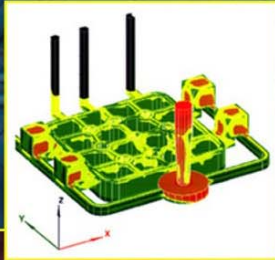
A fully integrated approach provides researchers with unique opportunities to address technologically related issues to solve metals processing problems and probe new technologies. Access is also available to 16 additional Oak Ridge National Laboratory (ORNL) user facilities ranging from state of the art materials characterization capabilities, high performance computing, to manufacturing technologies.

MPLUS can be accessed through a standardized User-submitted Proposal and a User Agreement. Nonproprietary (open) or proprietary proposals can be submitted. For open research and development, access to capabilities is provided free of charge while for proprietary efforts, the user pays the entire project costs based on DOE guidelines for ORNL costs.

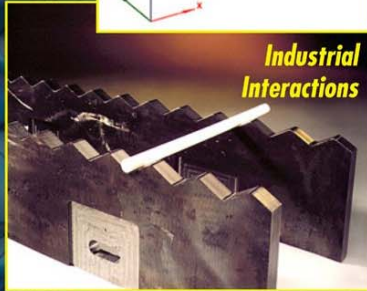
## METALS PROCESSING



### Casting and Solidification

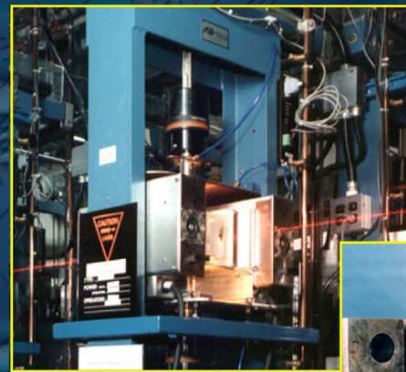


### Industrial Interactions

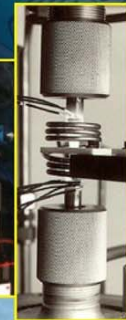


Castable and Weldable Intermetallics are being developed and implemented for industrial applications requiring high temperatures and corrosive environments.

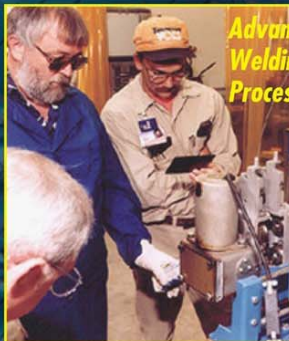
## METALS CHARACTERIZATION



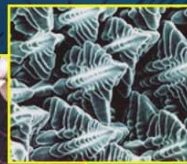
Innovative test methods are developed, and standardized ASTM and ASME codes are used to characterize materials and generate information for databases.



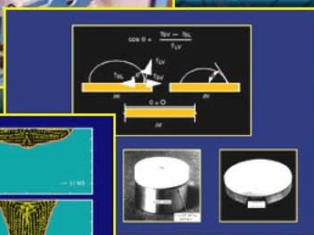
## METALS JOINING



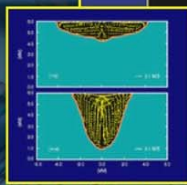
### Advanced Welding Processes



### Weld Metal Solidification



### Brazing of Metals and Ceramics

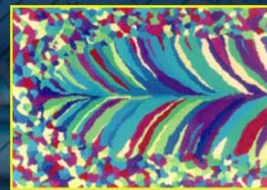


### Weld Modeling

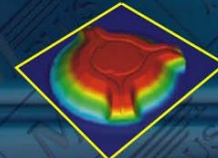
A wide range of conventional and advanced joining processes, weldability testing (including Gleeble™), brazing facilities (including those for characterizing wettability), and vision systems to view weld pool dynamics are available.

## METALS PROCESS MODELING

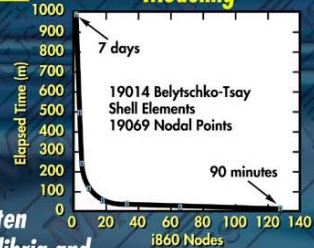
### Solidification



### Deformation



### Modeling



High-Performance Massively Parallel computer resources are coupled with computer models used to predict thermal gradients, molten metal flow, phase equilibria and

kinetics, solidification rates, strain distributions, residual stresses, etc.



### State-of-the-Art Dilatometry

Fig. 1. The MPLUS User Facilities.

## HIGHLIGHTS

---

The Materials Processing Laboratory Users (MPLUS) activity is an officially designated U. S. DOE, Office of Energy Efficiency and Renewable Energy, Industrial Technologies Program, Industrial Materials for the Future user facility at the Oak Ridge National Laboratory. The goal of MPLUS is to work with industries, universities, and other organizations in helping to meet the mission of Industries of the Future efforts. The MPLUS efforts are typically high risk feasibility research and development (R&D) activities that can help the development and implementation of new and emerging technologies. MPLUS projects can lead to improved understanding or show feasibility of materials technologies and processing methods in specific applications in various industries of the future areas. In this way the initial MPLUS results often identify significant materials issues and a path forward to improved energy, environmental, and economic benefits. There were 30 MPLUS user projects in FY 2001 and examples of energy benefits are presented below.

1. The Metals Processing Laboratory Users facility (MPLUS) study at ORNL with Logan Aluminum on Recycle Secondary Ingot (RSI) materials has led to new and significantly improved understanding of the role of RSI melting and casting practices on melt loss (dross formation). The study focused on the 5182 high magnesium-aluminum alloy used for producing can lid stock. At the Logan plant, approximately 75 million pounds/yr of RSI ingot are used for 5182 alloy production of which over one third was shown to be very high in dross content. The high dross content was found to be related to processing conditions during solidification of the RSI ingots—rapid cooling leads to low dross content and slow cooling leads to high dross content. Improving RSI solidification practice at recycle facilities or the elimination of high dross RSI at Logan can lead to an estimated energy benefit in the order of 0.34 trillion Btu/yr.

On a national level, the impact of these findings for 5182 aluminum alloy production could lead to energy savings of nearly 1 trillion Btu/year. Additional benefits would be expected in the production of other aluminum alloys containing high levels of magnesium.

2. The MPLUS effort on “Advanced Abrasion Resistant Materials for Mining” with Caterpillar determined the feasibility of post processing methods for fusing of coatings on non heat treatable carbon steels. These types of steels are used in earth moving equipment and experience both high wear and corrosion issues. The use of advanced coatings can improve energy benefits from the reduced wear and component usage, increased up time and less stoppage, and less frictional losses. Partly as result of this MPLUS project a proposal was submitted by Caterpillar that was approved. Energy impacts can lead to an estimated 0.5 trillion Btu/year.

3. The MPLUS effort with Weirton Steel on materials for use in Basic Oxygen Furnace (BOF) hoods focused on evaluating various types of alloys. BOF hoods are used for various functions including heat recovery; however, they often experience severe corrosion and wear issues. The MPLUS project identified various alternative materials for testing and evaluation. It was shown that the alternate materials could be applied to substrates or fabricated as tubes. A test panel was fabricated for evaluation at a steel mill. This effort also leads to the development and funding of a proposal submitted by the Energy Industries of Ohio focusing on BOF and Electric Arc Furnace (EAF) hoods. Weirton Steel is also participating in that project. Impact on steel making process could lead to an estimated energy benefit of nearly 4 trillion Btu/year.
4. The MPLUS effort on “Determination of True Stress-Strain Curves of Steels at Elevated Temperature” with Caterpillar focused on obtaining critical materials mechanical properties data that could be used in materials modeling efforts. This is important in order to reduce residual stresses and distortion in components. The MPLUS lead to a funded proposal on virtual weld-joint design with the goal of increasing weld joint service performance by 10 times and reducing energy use by 25 % through materials performance and productivity improvement using an integrated modeling process. Caterpillar uses 15 million pounds of weld wire per year and a 25% reduction would mean an estimated energy benefit of over 20 trillion Btu/year.
5. The MPLUS effort on “Fabrication, Heat-Treating Microstructures, and Tensile Testing of a High-strength 3Cr-3W-V(Ta) Alloy Plate” with Nooter Consulting Services focused on evaluating a new ORNL developed alloy, fabrication of alloy plates, and heat treating the plates in order to optimize the material’s microstructure. Nooter also evaluated the alloy in welding trials with and without heat treatment. The effort showed great results and also subsequently led to a funded project proposal. The development of the new alloy can have significant impact on various chemical processing components including, hydrocrackers, hydrotreaters, and industrial heat recovery systems. The successful implementation of Fe-3Cr-W(V) steel in chemical reactor components can result in estimated energy benefits of up to 21 trillion Btu/year.
6. The MPLUS effort on “Development of Seal Coatings for Ceramic Refractories for Molten Aluminum” with Pyrotek focused on evaluating the use of ceramics and processing methods for sealing the surface porosity in slip cast refractory tubes used for feeding molten aluminum in metalcasting operations. The effort included evaluating the feasibility of various ceramic slip systems, application of the various ceramics to the tubes, and heating/processing methods. The effort also led to a successfully funded project proposal by Pyrotek. The results of that project can impact the metalcasting, aluminum and glass industries in areas where the sealing of surface porosity of refractories is an important consideration especially in high temperature furnace and molten metal applications. The estimated energy benefits are nearly 15 trillion Btu/year.

Three MPLUS projects were performed with Alcoa related to the extrusion of aluminum. These projects yielded knowledge about the extrusion unit process and the impact of various variables on materials properties and process efficiencies. Alcoa is evaluating the results.

7. The project on “Rapid Preheating of Extrusion Dies” focused on evaluating rapid preheating technology of extrusion dies in an effort to accomplish real time changeover of extrusion dies without maintaining dies at temperature for a long period of time in a gas fired furnace (days). Infrared preheating technology was shown to be able to provide real time (less than 30 min) heating of dies for tool changing. An initial design of an IR furnace was also developed.
8. The project on “Improving the Surface Finishing of Extruded 6262 Alloy Billet” was performed in order to understand the reasons for material build up on die surfaces such that the efficiency of the process could be increased. As material builds up on the surface of extrusion dies, the surface quality of the aluminum part is severely impacted leading to scratches, loss in productivity, and resultant energy losses. Thermodynamic modeling of the aluminum alloy under the operational conditions indicated that the particles on the dies could very well be an extremely hard intermetallic alloy. Subsequent experimental measurements of the particles on the dies confirmed that the phase was indeed that calculated in the model. The analyses showed that the 6262 alloy contained a large number of hard particles rather than soft phases. The surface finish of the extruded aluminum is directly related to the size and amount of hard particles sticking to the dies. These results can be used to improve the efficiency of the process.
9. The project on “Energy Savings during the Extrusion of 6061 Alloy” focused on evaluating whether forced air cooling of extruded aluminum is necessary. The project evaluated the effect of cooling rate on the microstructure and the mechanical properties of the extruded billets. The results indicated that the forced fan cooling of the aluminum extrusions may not be necessary; thus leading to energy efficiency improvements.





**MPLUS No.:** MC-01-001

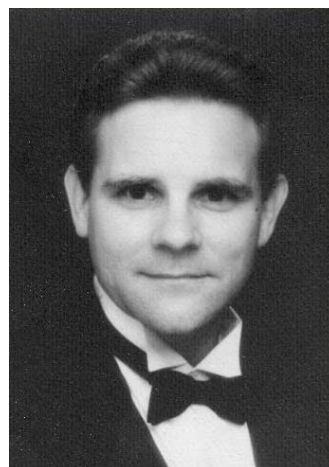
**Title:** Stress Analysis in Thin Surface Layers

**User Organization:** Vista Engineering Inc.  
Birmingham, AL 35226

**User Contact:** R. Thompson, 205-222-7419  
[rthompson@vistaeng.com](mailto:rthompson@vistaeng.com)

**ORNL R&D Staff:** B. Radhakrishnan, 865-241-3861  
[radhakrishnb@ornl.gov](mailto:radhakrishnb@ornl.gov)

**Relevance to OIT:** Chemical



Raymond Thompson from  
Vista Engineering Inc.

**Objective:** It was proposed to develop a stress analysis methodology to predict residual stress in diamond thin films deposited on a steel substrate. Thermal expansion mismatch between diamond and steel is such that cooling from the CVD process temperature of  $\sim 800^{\circ}\text{C}$  caused sufficient residual stress to spall the diamond film, which is typically 5 to 10  $\mu\text{m}$  thick. In order to eliminate spalling, several transition or buffer layers made up of carbides or nitrides are used. The residual stresses at these buffer layers were calculated. The results were used to optimize the design of the transition layers.

**Results:** The substrate material was 430 stainless steel. The buffer consisted of either a single layer of titanium nitride (TiN) or a double layer of TiN and tantalum carbide (TaC). The following parametric studies were conducted to determine the influence of the buffer layer thickness and the thickness of the diamond film on the stress normal to the various interfaces.

1. Effect of varying the diamond film thickness: Three different film thicknesses, 1, 3, and 9  $\mu\text{m}$  were modeled. The thickness of the buffer layer of TiN was kept constant at 3  $\mu\text{m}$  and the thickness of the steel layer was 50  $\mu\text{m}$ .
2. Effect of varying the thickness of buffer layer: Three different buffer layer thicknesses, 1, 3, and 9  $\mu\text{m}$  were modeled. The diamond film thickness was kept constant at 3  $\mu\text{m}$  and the thickness of the steel layer was 50  $\mu\text{m}$ .
3. Effect of introducing an additional buffer layer: An additional buffer layer of TaC was introduced and the influence of varying the thickness of TaC layer was modeled. Again, 1-, 3-, and 9- $\mu\text{m}$ -thick TaC layers were modeled with the thicknesses of diamond and TiN layers remaining constant at 3  $\mu\text{m}$ . The steel layer was also kept constant at 50  $\mu\text{m}$  for all these runs.

Increasing the diamond film thickness decreased the compressive stress on the diamond film. For a diamond film thickness of 9  $\mu\text{m}$ , the stress in the nitride buffer layer changed from compressive to tensile. The buffer layer thickness did not significantly affect the residual stresses. Increasing the thickness of the second buffer layer with different thermal expansion properties decreased the compressive stress on the diamond film. These results were incorporated in a diamond growing facility at Vista Engineering to produce good quality diamond films on steel substrates.

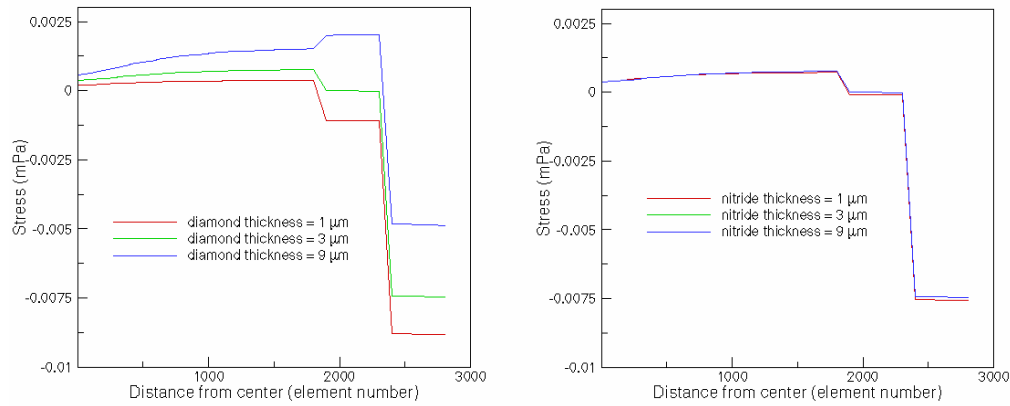


Fig. 1. Effect of varying diamond film thickness on radial stress, for a buffer layer thickness = 3.0  $\mu\text{m}$  (left) and effect of buffer layer thickness on radial stress for a diamond film thickness = 3  $\mu\text{m}$  (right).

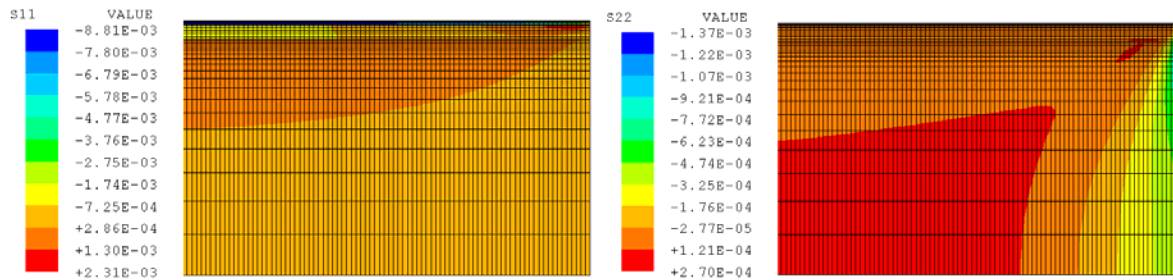


Fig. 2. Effect of diamond film thickness on radial (left) and axial (right) stresses on a cylindrical sample. Nitride buffer layer = 3  $\mu\text{m}$ ; diamond film thickness = 1  $\mu\text{m}$ .



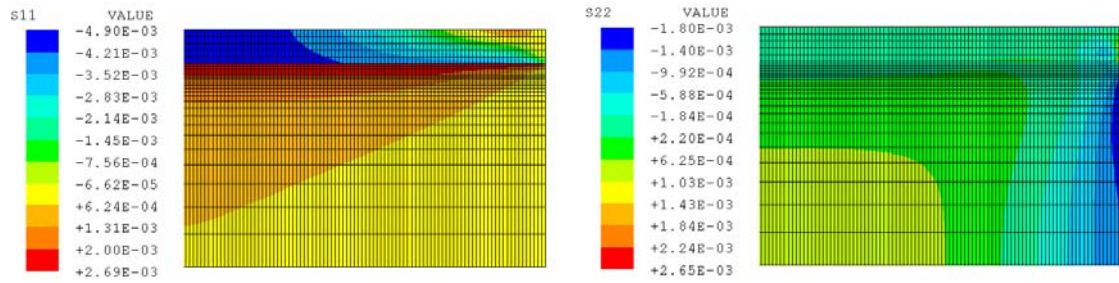


Fig. 3. Effect of diamond film thickness on radial (right) and axial (left) stresses on a cylindrical sample. Nitride buffer layer = 3  $\mu\text{m}$ ; diamond film thickness = 9  $\mu\text{m}$ .

### Reports/Publications/Awards:

B. Radhakrishnan, "Analysis of Stresses in Diamond Thin Film," MPLUS report, 2001.



**MPLUS No.:** MC-01-003

**Title:** Development of Infrared Thermal Processing Techniques for Improving the Wear and Corrosion Resistance of Coatings

**User Organization:** Caterpillar Inc.  
Peoria, IL 61656-1875

**User Contact:** M. Brad Beardsley, 309-578-8514  
[Beardsley\\_M\\_Brad@cat.com](mailto:Beardsley_M_Brad@cat.com)

**ORNL R&D Staff:** Gail M. Ludtka, 865-576-4652  
[ludtkagm@ornl.gov](mailto:ludtkagm@ornl.gov)

**Relevance to OIT:** Mining, Heat Treating

**Objective:** The goal of this MPLUS project was to determine the feasibility of a post-processing infrared heating methodology for fusing wear- and corrosion-resistant coatings onto representative non-heat-treatable carbon steels. The nine proprietary coatings were applied utilizing one of the following three different processes: (1) wire arc, (2) plasma spray, and (3) high velocity oxy-fuel (HVOF) spraying on cast iron and two different classes of steels. The substrate steel was carbon steel (1008 with approximate hardness of RB 90). Coating thickness ranges evaluated were: (1) 0.5 to 1.0 mm thick, or (2) 1 to 2 mm thick. These coatings then were evaluated and characterized via optical and scanning electron microscopy and microhardness indentation.

**Results:** An average increase of 95% was achieved in cross-sectional hardness for nine thermally sprayed, and infrared, plasma arc fused proprietary coatings. A metallurgical bond was achieved with four of these coatings. Coating chemistry, wetting characteristics, and preheating process parameters were determined to play significant roles in achieving successfully fused and bonded coatings.

Within the range of fusing parameters investigated, coatings up to approximately 1.2 mm in thickness could be fully fused and a metallurgical bond created at the coating-substrate interface.



Trent Weaver from Caterpillar Inc. watches as his coatings are being fused utilizing ORNL's one-of-a-kind 330-kW plasma-arc lamp.

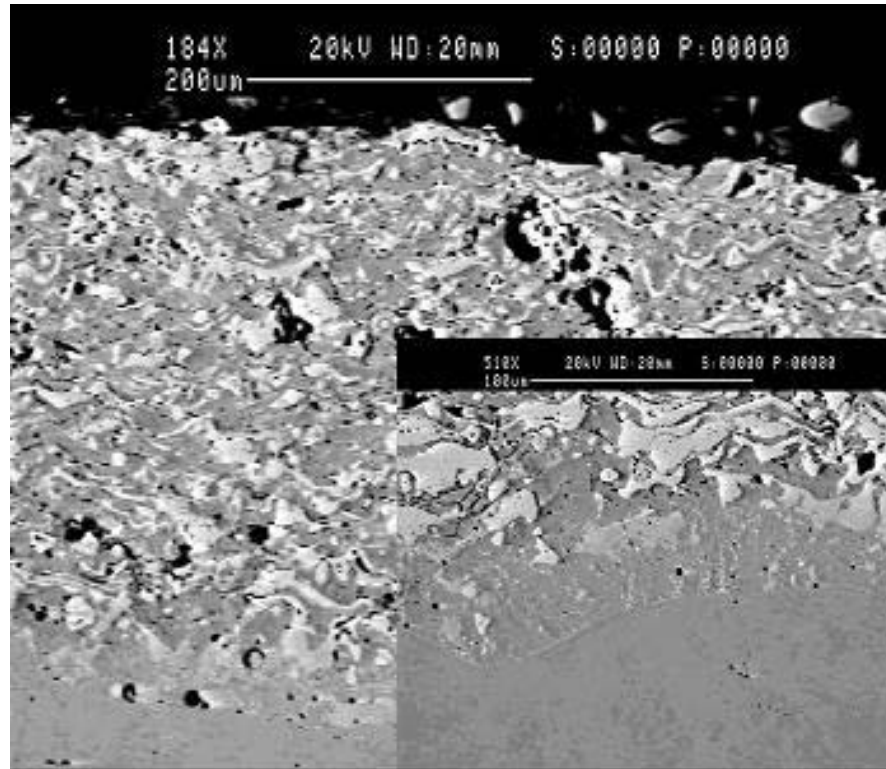


Fig. 1. Scanning electron microscope backscattered electron (SEM BSE) image of a composition coating. Inset is SEM BSE image of the coating bond line.

**Reports/Publications/Awards:**

D. T. Weaver, C. A. Blue, and Gail M. Ludtka, "Arc Lamp Treatment of Thermal Spray Coatings," MPLUS report, July 2001.

**MPLUS No.:** MC-01-004

**Title:** The Effect of Thermal Process Parameters on the Phase Transformation Behavior in Fully Austenitized, Medium-Carbon Alloy Steel

**User Organization:** Ispat Inland, Inc.  
East Chicago, IN 46312



Ispat Inland, Inc.  
East Chicago, Indiana

**User Contact:** Gopal R. Nadkarni, 219-399-5661  
[gnadk@ispat.com](mailto:gnadk@ispat.com)

**ORNL R&D Staff:** Gerard M. Ludtka, 865-574-5098  
[ludtkagm1@ornl.gov](mailto:ludtkagm1@ornl.gov)

**Relevance to OIT:** Steel, Heat Treating

**Objective:** Determination of the transformation kinetics of steels are crucial for understanding microstructural evolution, residual stresses, and shape changes of bar and rod materials made from steel. The intent of this MPLUS project was to characterize the phase transformation kinetic behavior and dilation strains of a high-strength, medium-carbon steel (SAE-AISI 1050) that had been fully transformed to austenite and then continuously cooled for a broad range of cooling rates. In addition this same alloy was heated into the austenite phase field and rapidly down-quenched below the eutectoid temperature and isothermally held at intermediate temperatures to determine the transformation times necessary for the various possible phase transformation sequences to go to completion under isothermal conditions.

**Results:** Figure 1 demonstrates the influence of cooling rate on the transformation temperatures and strains for this medium-carbon, low-alloy steel. The slowest cooling rate tested was 0.5°C/s and represents the curve with the highest transformation temperature (right-most curve) and coincides with formation of the equilibrium ferrite plus pearlite transformation sequence. As the cooling rate is steadily increased, the phase transformation upon cooling initiates at successively lower temperatures and indicates the transition of the austenite phase decomposition to the metastable microstructures of ferrite plus bainite and finally only the martensite phase at the fastest cooling rate of 170°C/s.

These quantitative data clearly show that the magnitude of the phase transformation dilation strain is very dependent on the microstructure that evolves which in turn is very dependent on the thermal transient upon cooling. Although not shown here, these transformation data were also recorded as a function of time to capture the transformation kinetics that are crucial for understanding the microstructure evolution in

the final bar and rod product. Modeling of product shape change during heat treatment will be critically dependent on capturing this behavior in the heat treatment simulation models. Similarly, the residual stress distribution developed in this material will be very dependent on the time and temperature dependent phase transformations that are occurring along with their respective dilation strains during cooling.

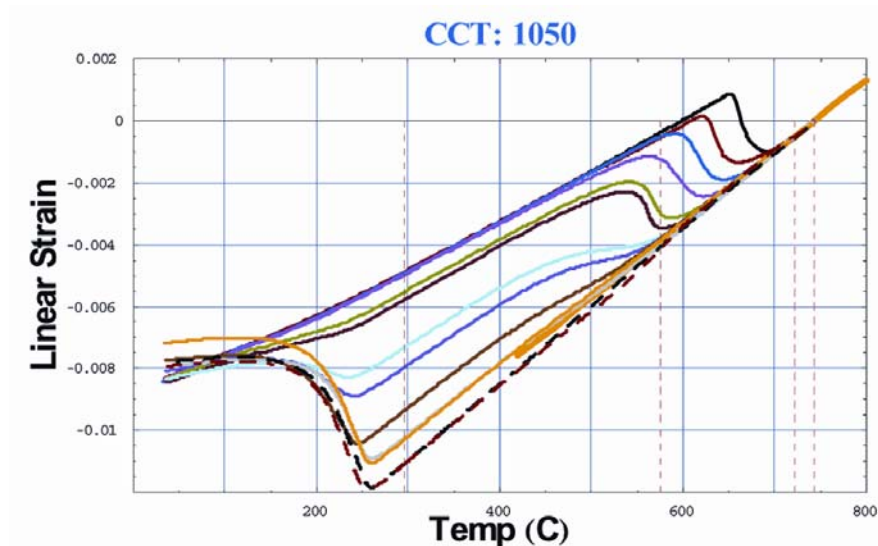


Fig. 1. Phase transformation dilation strain as a function of temperature for several controlled cooling rates obtained using the ORNL MPLUS high-speed quenching dilatometry facility.

The intermediate cooling rate continuous cooling curves depicted in Figure 1 also demonstrate that partitioning of the carbon solute is occurring for those transformation sequences that result in mixtures of bainite plus martensite at room temperature. This is evidenced by the lower martensite start temperatures observed under these conditions in contrast to that seen for the fastest cooling rate condition (lowest and left most curve). Higher carbon levels are associated with lower martensite start and finish temperatures. The carbon partitioning occurs during the formation of the bainite microstructure prior to initiation of the martensite transformation reaction.

Although not shown in this brief report, the isothermal phase transformation behavior of this material was also characterized to capture this information for future process modeling simulation purposes to predict the normalization heat treatment and forging behaviors of this SAE-AISI 1050 grade steel.

#### **Reports/Publications/Awards:**

G. M. Ludtka and G. R. Nadkarni, "The Effects of Thermal Process Parameters on the Phase Transformation Behavior in Fully Austenitized, Medium-Carbon Alloy Steel," MPLUS report, December 2002.

**MPLUS No.:** MC-01-005

**Title:** Recovery Boiler Wall Tube Temperature Measurements

**User Organization:** Babcock & Wilcox  
Barberton, OH 44203

**User Contact:** John Kulig, 330-860-6438  
[jakulig@pgg.mcdermott.com](mailto:jakulig@pgg.mcdermott.com)



Gorti Sarma (left) from ORNL with John Kulig from Babcock & Wilcox

**ORNL R&D Staff:** Gorti Sarma, 865-574-5147, [sarmag@ornl.gov](mailto:sarmag@ornl.gov)  
Jim Keiser, 865-574-4453, [keiserjr@ornl.gov](mailto:keiserjr@ornl.gov)

**Relevance to OIT:** Forest Products, Process Heating

**Objective:** It is being noted that the lower walls of black liquor recovery boilers in Kraft paper mills are experiencing severe corrosion and/or cracking in some locations. To better define the condition of the tubes at the time this degradation is occurring, a number of thermocouples have been mounted on wall tubes in a boiler that has experienced severe tube degradation. The temperature data generated by these thermocouples, as well as boiler operating parameters, were collected and analyzed to determine if there is a relationship between periods when large temperature fluctuations are observed and some operating conditions.

**Results:** Thermocouple data were recorded at ten second intervals, so that a given day had up to 8640 values for each thermocouple location. Due to the complexity of the temperature variations on any given day, as well as the large quantities of data collected, it was felt that a more quantitative measure of the temperature fluctuations would be useful.

Count of number of high temperature data points: One of the simplest methods of identifying if a thermocouple is relatively calm or active is to count the number of data points recorded at that location which exceed a given critical temperature. Examination of data during relatively “calm” periods indicated the “baseline” operating temperature to be between 325 and 375°C. Earlier work on modeling the cooling of floor tubes from operating temperature during boiler shutdown suggested that a temperature drop of about 75°C is sufficient to cause the stress at the crown of the 304LSS composite tube to change from compressive to tensile yield. Based on this result, and considering a temperature increase of 75°C above the upper limit of the “baseline” operation regime to be critical, any temperature value above 450°C was determined to be a “thermal excursion,” and a count of the number of such “excursions” was made for each

thermocouple. Figure 1 shows the results of the thermal “excursion” count for the thermocouple at position 2 on air port F4 (#4 on the front wall) for the month of May 2001. The first few days shows a number of active days with high numbers of “excursions.”

Count of number of half-cycles: Among the possible causes for cracking of air port tubes are thermal fatigue and corrosion fatigue, both of which require stress cycles. It therefore becomes necessary to estimate the number of fatigue cycles experienced by the tube. A half-cycle is defined as the increase or decrease in temperature of more than 75°C from the previous lowest or highest value, respectively. Any fluctuations in temperature less than 75°C are ignored, and the up- and down-cycles occur in sequence alternately. Figure 2 shows the plot of half-cycle count for the different thermocouples for May 2001. The number of half-cycles varies depending on both location of the air port in the boiler and location of the thermocouple at the air port.

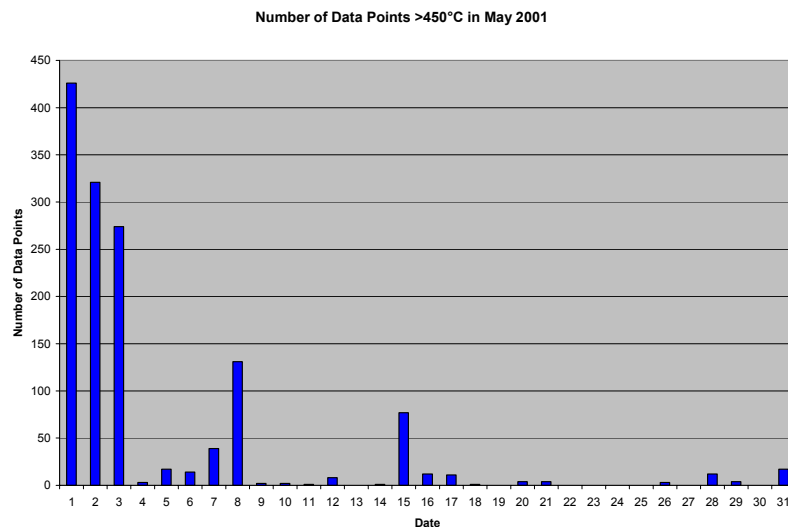


Fig. 1: Bar chart showing the number of thermal “excursions” above 450°C at F4-2 during May 2001.



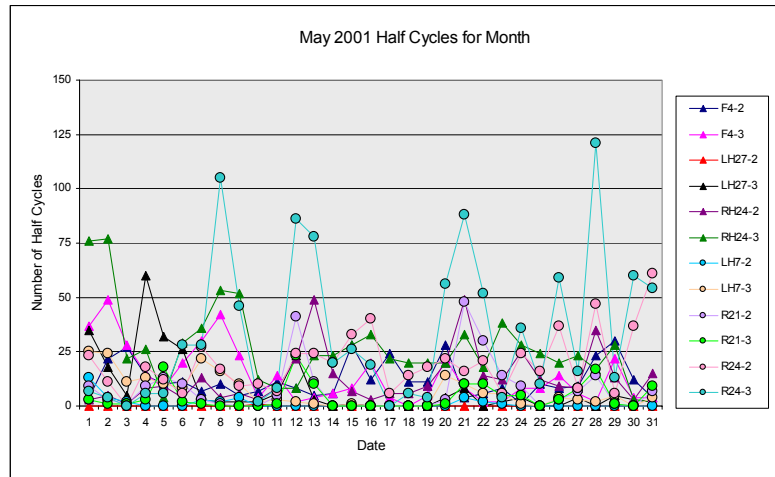


Fig. 2: Half-cycle count based on data collected during May 2001 at the different thermocouple locations.

### Reports/Publications/Awards:

G. B. Sarma, K. A. Choudhury, J. R. Keiser, F. E. Steinmoeller, K. B. Rivers, C. M. Mackenzie, B. B. Stone, and J. A. Kulig, "Recovery Boiler Wall Tube Temperature Measurements," MPLUS report, January 2002.



**MPLUS No.:** MC-01-006

**Title:** Analyses of Weld Overlay Tubes

**User Organization:** Babcock & Wilcox  
Barberton, OH 44203

**User Contact:** Joan Barna, 330-860-6766  
[jlbarna@babcock.com](mailto:jlbarna@babcock.com)



Gorti Sarma (left) from ORNL with  
John Kulig from Babcock & Wilcox

**ORNL R&D Staff:** Gorti Sarma, 865-574-5147, [sarmag@ornl.gov](mailto:sarmag@ornl.gov)  
J.R. Keiser, 865-574-4453, [keiserjr@ornl.gov](mailto:keiserjr@ornl.gov)

**Relevance to OIT:** Forest Products, Welding

**Objective:** Kraft recovery boilers are used by the pulp and paper industry to burn black liquor for recovering certain chemicals that are subsequently used in the paper making process. The floor and walls of the recovery boilers are made of composite tubes with an inner SA210 carbon steel layer and an outer layer of a more corrosion-resistant material such as Alloy 625. It is known that the floor tubes are subjected to temperature fluctuations during the operation of the boiler. The proposed research is aimed at performing thermal and mechanical analyses of the tubes on the boiler floor under different scenarios, including a normal operating cycle and the presence of temperature excursions of different magnitudes. The goal is to determine the variations in the stress state in the Alloy 625/SA210 composite tubes when the outer clad layer is applied using a weld overlay process. This problem is of great importance, since presence of tensile stresses in the tube can cause stress corrosion cracks to develop in the tubes due to the corrosive operating environment.

**Results:** Modeling was carried out using the finite element program ABAQUS, to analyze the changes in stress components in the composite floor tubes and membranes due to changes in temperature during boiler operation. A 2-D model was used to analyze the welding process to join the tube and membrane, and results were used in a 3-D model of a floor tube panel under various operating conditions. The stresses in the tube and membrane are altered by temperature gradients and differences in material properties between the clad layer and carbon steel.

Neutron and X-ray diffraction measurements showed that tubes made by co-extrusion, as well as tubes subjected to heat treatment after the weld overlay process have negligible residual stresses. After welding to make the panels, axial stresses are compressive and hoop stresses are tensile at the crown of the tube. These stresses undergo only small changes during heating and return to initial values upon shutdown, due to the similar thermal expansion mismatch properties of Alloy 625 and carbon steel. At the center of the membrane, the axial stresses are tensile and hoop stresses are compressive in both materials, and they remain so during the cycle. Tensile axial

stresses can cause transverse cracks in the membrane to propagate paste the interface into the carbon steel later.

Analyses of temperature excursion: In addition to a normal operating cycle, effect of a localized thermal spike to 480°C was analyzed. At the fireside tube crown, the temperature excursion leads to yielding in Alloy 625, causing the axial stress to become tensile on return to operating temperature. Cooling to room temperature causes further increase in magnitude of tensile stress. The hoop stress also remains highly tensile, as shown in Figure 1. The stress variation on the carbon steel side of the interface shows a similar trend, with compressive axial stress becoming tensile after the thermal spike and remaining tensile during a subsequent normal operating cycle.

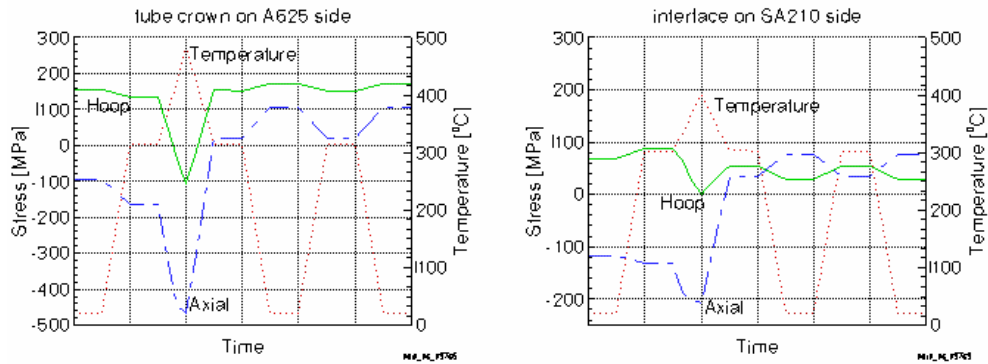


Fig. 1: Stress variation at the tube fireside crown during an operating cycle that includes a thermal spike to 480°C.

Analyses of panel heat treatment: In order to see if heat treatment of the panel would be beneficial in reducing the stresses, heating of the panel to 900°C, followed by cooling to room temperature was modeled, followed by a normal operating cycle. At the tube crown, the axial stress becomes more compressive and the hoop stress becomes less tensile in the Alloy 625 layer, as shown in Figure 2. In the carbon steel layer, the magnitude of the stress components becomes almost zero. At the center of the membrane, there is little change in the tensile axial stress, but the transverse stress becomes less compressive in the clad layer, while the stresses become close to zero in the carbon steel layer.

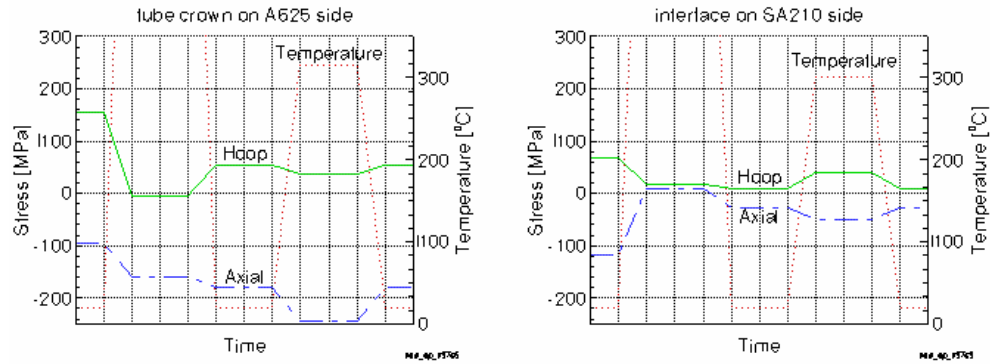


Fig. 2: Stress variation at the tube fireside crown during a normal operating cycle after heat treatment of the panel at 900°C.

### Reports/Publications/Awards:

G. B. Sarma, J. R. Keiser, F. E. Steinmoeller, K. B. Rivers, C. M. Mackenzie, B. B. Stone, and J. A. Kulig, "Analyses of Weld Overlay Tubes," MPLUS report, January 2002.



**MPLUS No.:** MC-01-007

**Title:** Investigation of Oxidation of Superalloys at High Pressures and Temperatures

**User Organization:** GE Aircraft Engines  
Cincinnati, OH 45215

**User Contact:** Ben Nagaraj, 513-786-2287  
[ben.nagaraj@ae.ge.com](mailto:ben.nagaraj@ae.ge.com)

**ORNL R&D Staff:** P. F. Tortorelli, 865-574-5119  
[tortorellipf@ornl.gov](mailto:tortorellipf@ornl.gov)

**Relevance to OIT:** Combined Heat and Power

**Objective:** The objective of this MPLUS project was to investigate the effect of pressure on the oxidation of nickel-based superalloys.

**Results:** The ability of ORNL to conduct specialized experiments at high pressures as well as high temperatures was utilized in this project to examine the oxidation of several superalloys. Rectangular superalloy coupons, approximately  $2.5 \times 2.5 \times 0.2$  cm, were mounted on an alumina specimen holder, as shown in Figure 1, and exposed to dry air at 15.6 atm for 54 h at either 730 or 845°C. Gravimetric results are shown in Figures 2 and 3. Overall, the oxidative mass changes were low despite the high gas pressure. Data reproducibility was good and consistent with little, if any, oxide spallation. Overall, the oxidative mass changes were low despite the high gas pressure. Little difference in oxidation rate over 54 h was observed for the three superalloys at 730°C (Figure 2). However, at 845°C, Rene 80 showed significantly less oxidation resistance than Rene 142 and alloy 625 (Figure 3).



Ben Nagaraj from GE Aircraft Engines holding furnace tube against measuring stick.

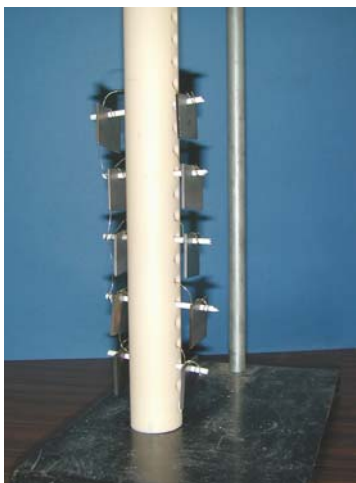


Fig. 1. Rectangular superalloy coupons mounted on an alumina specimen holder.

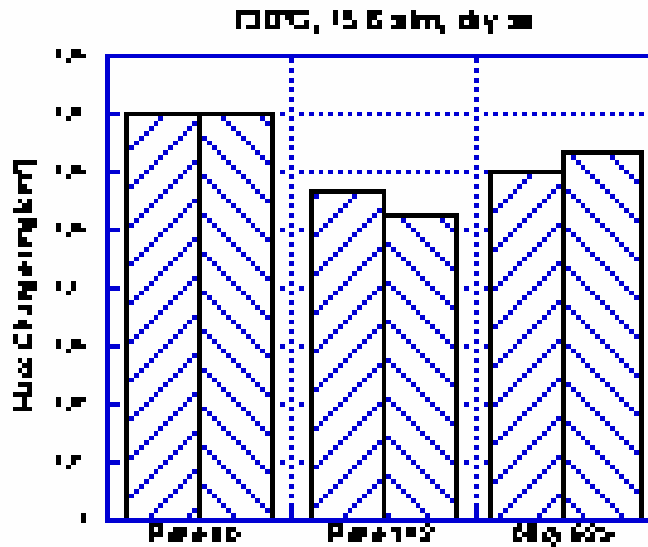


Fig. 2. Gravimetric results. Little difference in oxidation rate over 54 h was observed for the three superalloys at 730°C.

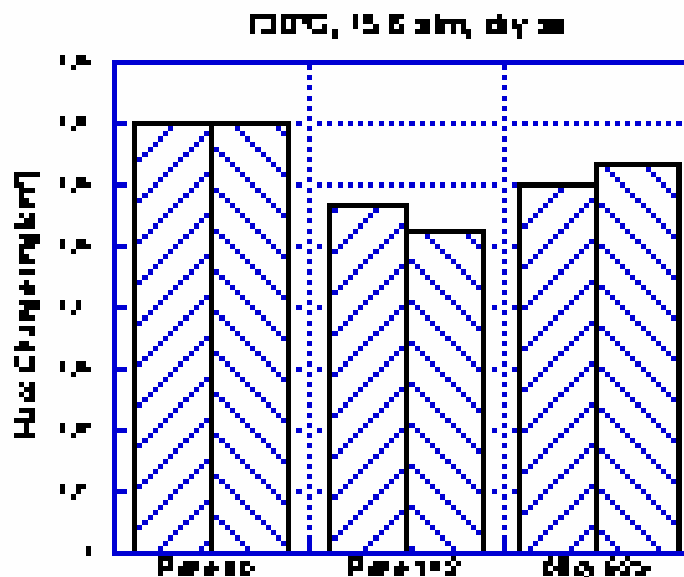


Fig. 3. Gravimetric results. At 845°C, Rene 80 showed significantly less oxidation resistance than Rene 142 and Alloy 625.

#### Reports/Publications/Awards:

Peter Tortorelli and Ben Nagaraj, "Investigation of Oxidation of Superalloys at High Pressures and Temperatures," MPLUS report, January 2003.



**MPLUS No.:** MC-01-009

**Title:** Evaluation of Filler Metals for Improved Elevated Temperature Strength of Aluminum Welds

**User Organization:** Eagle Racing  
Loudon, TN 37774

**User Contact:** Michael R. Hedgecock, 865-408-1000  
[eagleracin@aol.com](mailto:eagleracin@aol.com)

**ORNL R&D Staff:** Jim F. King, 865- 574-4807  
[kingjf@ornl.gov](mailto:kingjf@ornl.gov)

**Relevance to OIT:** Welding, Metalcasting, Aluminum



Michael R. Hedgecock from  
Eagle Racing

**Objective:** Eagle Racing sought to determine if improvements were possible for extending the service life of repair welded aluminum engine heads used in NHRA Drag Racing. Examination of the heads had revealed failure due to extreme overheating and deformation around valve seats in nitro-methane fueled engines. It was desirable to achieve additional high temperature strength in repair welds at these locations. Extruded aluminum billets with machined grooves were evaluated for general weldability and subsequent evaluation of weld deposit strength. The grooves were welded using the gas-tungsten-arc (GTA) welding process that was typical of Eagle's repair technique. Two welding filler metals were evaluated, one that was the standard used in Eagle Racing's applications and a commercially available 'high-strength' filler metal. Weld specimens were evaluated metallographically. Additional weldments were also produced at ORNL for comparison. These were evaluated by metallographic examination and hardness testing of the deposit in the as-welded condition and after heat treatment. Specimens of the welds were given either a standard aluminum heat treatment, tested as welded, or after surface peening.

**Results:** The weldment samples were typical of repair welds produced during the rebuilding of aluminum engine heads. The weldments were produced with the gas tungsten arc process using 4043 filler metal (Weldment 1), which was the standard alloy, and 5356 filler metal (Weldment 2) that was suggested during this project as an alternate with the potential for higher strength. Weldment 3 was made with 5356 filler metal and had been surface peened with a hammer immediately after welding. These weldments were examined metallographically.

Weldment 1, 2, and 3 were found to be similar in that all contained scattered porosity and cracking along the fusion line. Figure 1 illustrates these discontinuities that were found in Weldment 1 with 4043 filler metal and this was considered the poorest quality weld deposit of the submitted samples. The Weldment 2 sample with 5356 filler metal contained less porosity and was of slightly better quality, Figure 2.

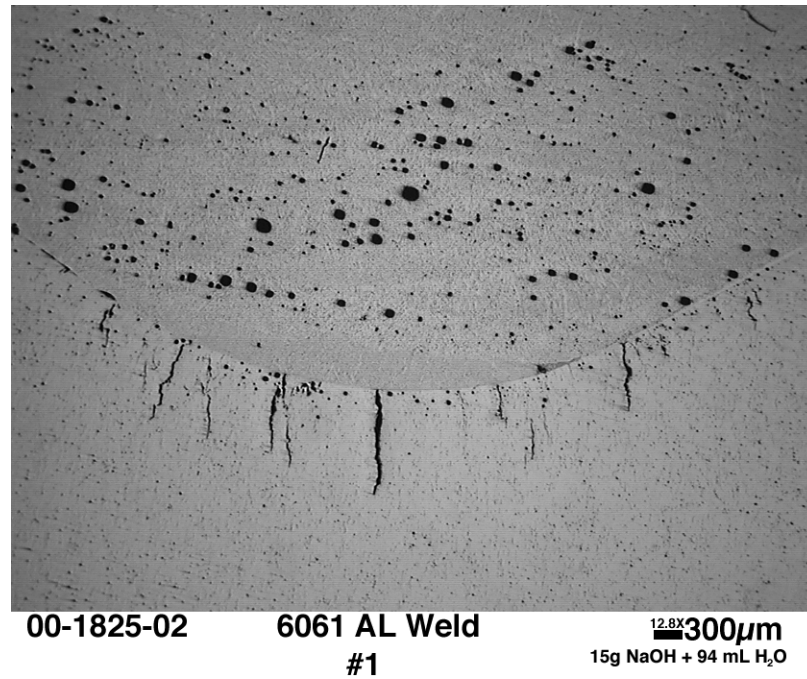


Fig. 1. Standard 6061 aluminum engine head weld repair technique with 4043 filler metal contained fusion line cracking and scattered porosity.

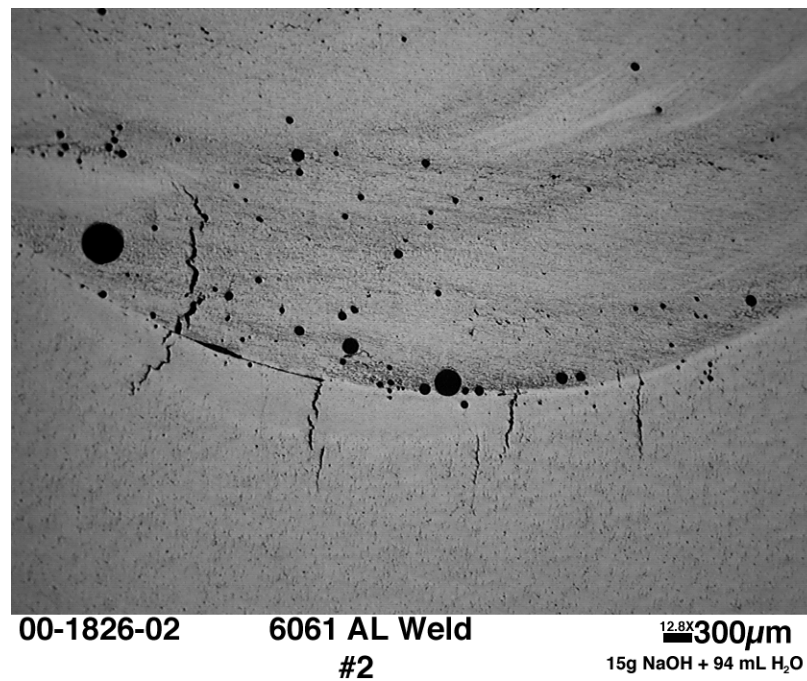


Fig. 2. Engine head repair weld made with 5356 filler metal contained less porosity than 4043 weldment.

Based on these results, similar weldments were made at ORNL for additional testing. Filler metals 4043, 4643, 5356, and an experimental Al-Si alloy were deposited with the GTA process. Gas metal arc (GMA) weldments were made with a few of these alloys. It was determined that GMA did not offer a satisfactory improvement in weld quality and its use was not recommended. Rockwell B hardness measurements were made on sections of the as-welded deposits and after thermal aging at 350°F for 18 hours for the 5356 alloy. The 5356 filler metal had higher hardness, RB 64 compared to RB 50 for the 4043. The thermal aging had only a minor improvement in hardness. This is compared to the 6061-T6 base metal hardness of 100RB.

It was concluded that 5356 had higher hardness, and therefore higher strength, than the 4043 previously used under these conditions. Additionally, it was found to have better machining properties that improved the head finishing operation. The GTA welding process currently used is the best choice. Mechanical surface peening did not appear to offer any improvement in properties. It was determined that weldment hardness and strength could not be achieved that matched the base metal, so the 5356 filler used in the as-welded condition offers the best choice for this application. The extremely high temperature and pressures present in these racing engines subjects any weld repaired aluminum engine head to stresses near its limit.

#### **Reports/Publications/Awards:**

J. F. King, Letter Report of Analysis to Mike Hedgecock at Eagle Racing, October 17, 2002.



**MPLUS No.:** MC-01-010

**Title:** Pyrowear 53: Dilatometry to Determine Phase Transformation Kinetics

**User Organization:** Deformation Control Tech.  
Cleveland, OH 44130

**User Contact:** Blake L. Ferguson, 440-234-8477  
[dictinc@compuserve.com](mailto:dictinc@compuserve.com)

**ORNL R&D Staff:** Gerard M. Ludtka, 865-574-5098  
[ludtkagm1@ornl.gov](mailto:ludtkagm1@ornl.gov)

**Relevance to OIT:** Heat Treating, Forging, Steel, Mining



Lynn Ferguson



Greg Petrus



Andy Freborg

**Objective:** Pyrowear 53, a carburizing steel, is used primarily for helicopter gear applications where toughness, fatigue strength, resistance to wear, and resistance to softening at elevated temperatures are important. It has not been well characterized in terms of transformation kinetics or mechanical behavior. In use, its high hardenability results in martensitic microstructures with some retained austenite. In practice, the gears are carburized, cooled to room temperature, re-austenitized, press quenched, and double or triple tempered with associated cryogenic treatments between tempering steps. Because of the presence of stable alloy carbides, resolutionizing of carbides is slow and not documented. The quenching response is not well documented. An incomplete isothermal transformation diagram and  $M_S$  and  $M_F$  temperatures for the base steel and a carburized case are available in the literature. In order to simulate heat treatment response for possible process improvement, cost reduction, or the design of new products or redesign of existing products, these material responses needed to be quantified.

In this MPLUS project, phase transformation dilatometry during heat-up, and austenitization documented heating kinetics and carbide dissolution kinetics were determined. Additionally, high-speed quenching dilatometry tests further documented martensite kinetics and dilations as a function of austenite carbon content, which is directly related to carbide dissolution during the initial austenitization cycle. These results will be incorporated into a phase transformation kinetics model for use in a predictive heat treatment simulation software tool, DANTE, to facilitate accurate simulation of microstructure, residual stress, and distortion evolution during heat treatment of the PYROWEAR 53 steel alloy.

**Results:** Because this alloy is normally used in the carburized condition, dilatometer samples first had to be carburized through its cross section so that a range of carbon levels could be characterized. The carbon levels used for this study included 0.1, 0.34, 0.52, and 0.81%. Carburization of 8-mm-diam tubular samples with a 1 mm wall

thickness was performed by a commercial heat treater, Horsburgh & Scott Company. Dilatometer samples in the through-carburized condition were provided to the Oak Ridge National Laboratory and tested on this MPLUS project. The samples were tubular, with an outer diameter of 8 mm, an inner diameter of 6 mm, and a length of 8 mm.

Results for both the 0.10% C and the 0.81% C specimens have indicated rapid solution of the carbon/carbides upon austenitization, with complete transformation to martensite even under air cooling conditions. For the 0.10% C material, an isothermal hold at 500°C, which is below the martensite start temperature ( $M_s$ ) of 510°C reported by the steel's producer, Carpenter Technology Corporation, and well below the reported ferrite/pearlite nose temperature of 700°C, did not result in any austenite decomposition and martensite formed upon subsequent cooling. The dilatometry data obtained from the production material reveals several very interesting and perhaps key findings. For example, one of the dilatometry curves obtained for the fully carburized (0.81% C) Pyrowear material that was heated to 913°C, held for 1 min (all carbon and carbides into complete solution) and cooled, indicates a  $M_s$  temperature of about 100°C, versus 130°C as reported in the Car-Tech data sheet.

Figure 1 shows a plot of a dilatometer curve for the baseline (0.10% C) material. This sample was heated to 1000°C and held for 1 min, achieving complete solution of the carbon/carbides, and then cooled. The plot shows several interesting phenomena. First, as was the case with the 0.81% C carburized sample, the  $M_s$  temperature was found to be 380°C, versus 510°C as reported in the Car-Tech product information. Also, a distinct volumetric expansion on heating occurs just prior to austenitization (indicated on plot). The nature of this phenomenon is not known, but it is present in all samples to some degree. The pattern was clearly seen in all eight noncarburized samples tested, and it appears somewhat "masked" in the carburized material. It is believed this phenomenon is most likely due to the high alloy content of the Pyrowear alloy.

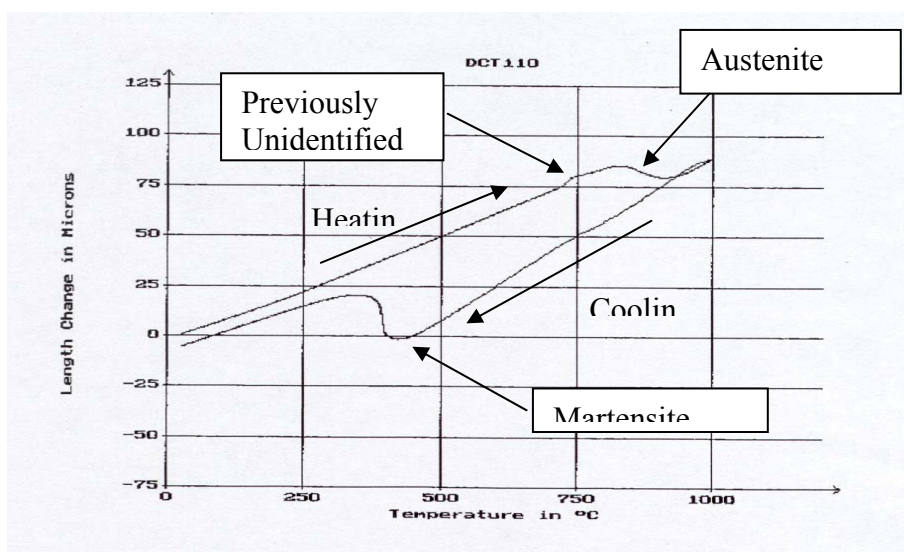


Fig. 1. Plot of a dilatometer curve for the baseline (0.10% C) material.

Thus the results indicate the following with respect to Pyrowear 53:

1. For both the carburized and noncarburized samples, the experimentally determined martensite start temperature was markedly lower than that reported by producer of the steel.
2. The noncarburized samples all displayed a distinct volumetric expansion on heating just prior to the austenite transformation. The phenomenon was reduced in the 0.80% carbon material.
3. An extended (17 h) isothermal hold at 500°C produced no discernable phase change as would be witnessed by a volumetric expansion. The martensite start temperature was likewise unaffected.

**Reports/Publications/Awards:**

B. L. Ferguson, Andrew Freborg, G. M. Ludtka, and W. Elliott, "Pyrowear 53: Dilatometry to Determine Phase Transformation Kinetics," MPLUS report, April 2002.





**MPLUS No.:** MC-01-011

**Title:** Dilatometric Study of Phase Transformation and Resultant Phase Fractions in Forged 1550 Steel for Comparison to and Definition of the Microstructures of Induction-Hardened Parts

**User Organization:** Cummins Engine Company  
Columbus, IN 47201

**User Contact:** Roger D. England, 812-377-7573  
[roger.d.england@cummins.com](mailto:roger.d.england@cummins.com)

**ORNL R&D Staff:** Gerard M. Ludtka, 865-574-5098  
[ludtkagm1@ornl.gov](mailto:ludtkagm1@ornl.gov)



Roger D. England from  
Cummins Engine Company

**Relevance to OIT:** Heat Treating, Forging, Steel

**Objective:** Current industry practice for induction hardening of steel alloy components has the potential to produce microstructure and property variability. Therefore, a complete knowledge of the effects of time and temperature on carbon and alloying element dissolution is essential to preventing undesirable component behavior. For this purpose, the high-speed quenching dilatometry facility at ORNL is a very time and cost efficient manner to accomplish this critical microstructural evolution characterization.

Accurate measurement of the transformation kinetics of ANSI 1550 steel under well known and controlled heat treatment conditions was needed. In particular, the thermal processing conditions required to achieve complete austenitization and subsequent formation of stable, martensitic microstructures upon quenching were to be determined, and the phase transformation behavior at various cooling rates and under isothermal transformation conditions was required. The resultant phase fractions present could then be compared to those that were present in induction-hardened parts. This has the potential to help Cummins Engine Company determine the actual thermal history of the gradient microstructures present in the induction-hardened parts.

**Results:** Because rapid induction heating and cooling does not allow the entire component to reach isothermal condition, this study examined the effects of variable austenitization times and temperatures on the resultant microstructures. Figure 1 exhibits a typical martensitic microstructure obtained under high-speed quenching at a cooling rate of 190°C/s (a T<sub>8/5</sub> of 1.59 s). Figure 2 shows the variability of the martensite start, M<sub>s</sub>, transformation temperature and total phase transformation dilation strain based on small changes in austenitization times and temperatures. The austenitization conditions used in this figure were: (1) 900°C for 10 min, (2) 950°C for

10 min, (3) 950°C for 5 min, and (4) 950°C for 5 s. The  $M_s$  temperatures determined ranged from 280 to 325°C, which can only be the result of different carbon dissolution into the austenite phase prior to quenching.

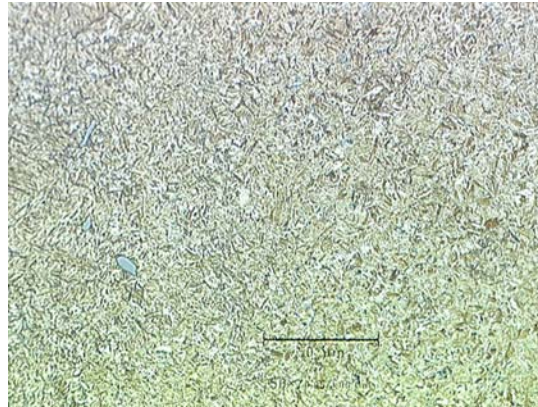


Fig. 1. Fully martensitic microstructure of steel alloy ANSI 1550. (Magnification marker represents 50  $\mu\text{m}$ .)

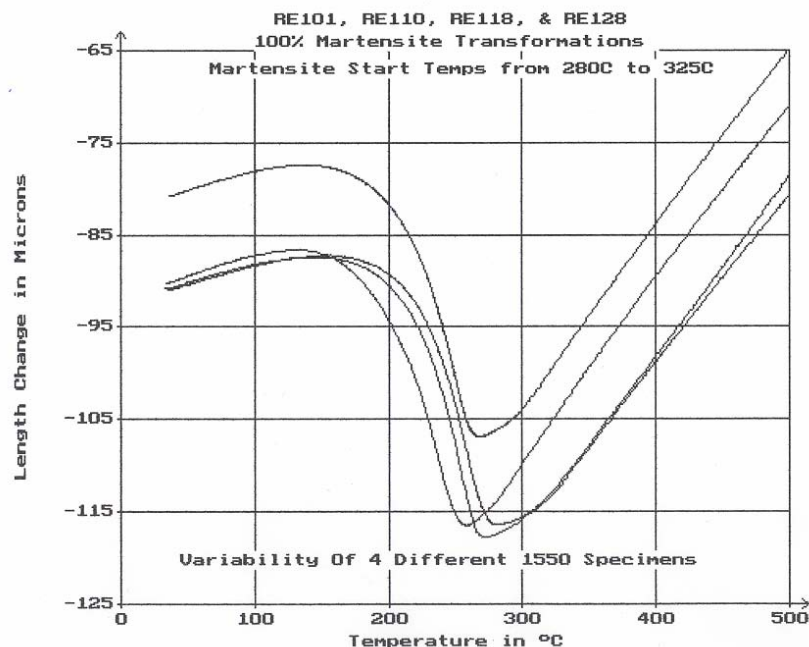


Fig. 2. Variability in Mg due to austenitization parameters.

### Reports/Publications/Awards:

G. M. Ludtka and R. D. England, "Dilatometric Study of Phase Transformation and Resultant Phase Fractions in Forged 1550 Steel for Comparison to and Definition of the Microstructures of Induction-Hardened Parts," MPLUS report, December 2002.

**MPLUS No.:** MC-01-012

**Title:** Detection of Fabrication Defects and Oxidation in Aluminum Recycled Scrap Ingots (RSI)

**User Organization:** Logan Aluminum  
Russellville, KY 42276

**User Contact:** John Zeh, 270-755-6502  
[john.zeh@logan-aluminum.com](mailto:john.zeh@logan-aluminum.com)

**ORNL R&D Staff:** Qingyou Han, 865-574-4352  
[hanq@ornl.gov](mailto:hanq@ornl.gov)

**Relevance to OIT:** Aluminum, Metalcasting



John Zeh from Logan Aluminum

**Objective:** The purpose of this MPLUS project was to evaluate aluminum recycled scrap ingots (RSI) in order to determine the extent of oxidation products in various types of RSI. Aluminum RSI is produced from recycled aluminum and is used as a significant fraction of feed material in aluminum melting furnaces (up to 25% of the total melt). The presence of oxidation products in aluminum RSI can lower the overall efficiency and recovery of aluminum. The objectives of this project were to: (1) evaluate various techniques such as high voltage X-ray transmission for detecting fabrication defects including dross oxidation products, and (2) performing a microstructural analysis of the RSI to relate any issues to processing.

**Results:** X-ray and ultrasonic techniques were used to detect defects in aluminum ingots. Defects as large as a one cent coin could be detected but no large dross particles were found in aluminum 5182 RSI. The project then concentrated on determining why a large amount of dross was observed during the remelting of the ingot. Samples were taken from the center of the ingot and the microstructure of the specimens was characterized. Melting experiments were carried out with surprising results. The specimens taken from the center of the aluminum 5182 RSI could not be melted at 850°C, about 212°C degree higher than the liquidus temperature of the alloy. Figure 1 shows the specimens after being held at 850°C for 26 h. The specimens were semi-solid but did not collapse at such a high temperature of more than 212°C higher than its melting point. This represented a very large fraction of aluminum that oxidized.



Fig.1. Specimens hold at 850°C for 26 h.

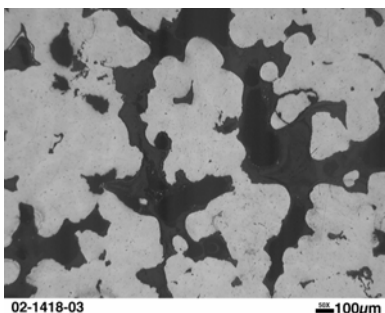


Fig.2. Microstructure of the dross.

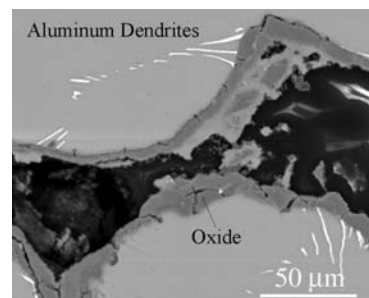


Fig.3. Scanning electron microscope image of the dross.

Aluminum liquid collected at the bottom of the crucible, and the dross ratio (the ratio of the weight of oxide to that of the specimen) was determined. The dross ratio for various specimens ranged from about 50 to 80%, meaning that more than 50% of aluminum in the center of the RSI had been oxidized.

The microstructure of the dross was then characterized. Figure 2, taken on as-polished surface of the dross, shows the presence of aluminum dendrites and pores. The scanning electron microscopy (SEM) image shown in Figure 3 revealed that the surfaces of the aluminum dendrites were covered with a layer of oxide. It was concluded that the oxide-reinforced structure prevented the specimen from collapsing at a temperature of 850°C. As a result, the aluminum liquid was entrained in a solid oxide shell. A large fraction of aluminum metal was thus being oxidized during the process of producing residual secondary ingots.

In order to determine the origin of the oxide layer, the as-cast microstructure of the various RSI specimens was characterized. As illustrated in Figure 4, severe interdendritic pores occurred between dendrites. The microstructure of the ingot was found to be identical to that of the dross. A layer of oxide was found on the surfaces of the interdendritic pores, Figure 4. This indicated that the oxide layer was formed during solidification of the RSI. It is suggested that the reduced pressure at the center of a solidifying RSI, due to solidification shrinkage, incorporates air into the center of the RSI through the pathways comprised of interdendritic pores and cracks, leaving oxide on the surfaces of the interdendritic pores.

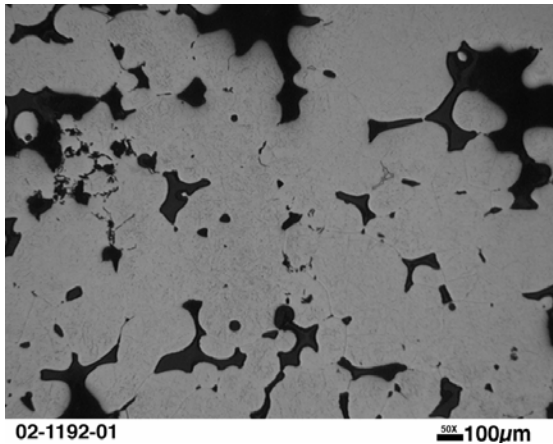


Fig. 4. The as-cast microstructure of specimen taken from the center of a RSI shows a high degree of porosity.

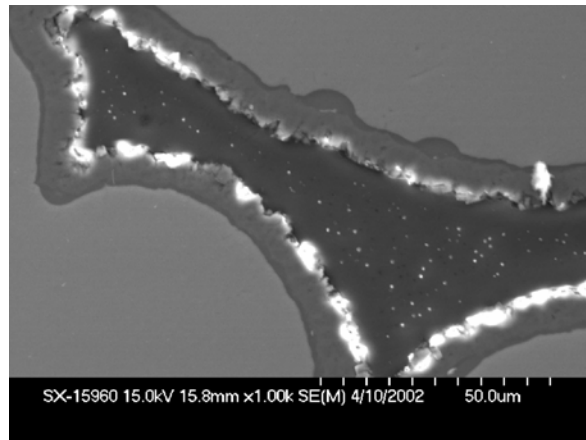


Fig. 5. The SEM image of as-cast microstructure shows the presence of oxide on the surface.

#### Reports/Publications/Awards:

W. A. Simpson, Q. Han, and J. Zeh, "Detection of Fabrication Defects in Aluminum Sows," MPLUS report, May 2002.

Q. Han, W.A. Simpson, J.L. Zeh, E.A. Kenik, and V.K. Sikka, "The Effect of Solidification Defect on the Dross Formation during Re-melting of Aluminum 5182 Alloy RSI," *Light Metals 2003*, accepted for publication.

Q. Han, W.A. Simpson, J.L. Zeh, E. Hatfield and V.K. Sikka, "Dross Formation during Remelting of Aluminum 5182 Remelt Secondary Ingot (RSI)," submitted to *Metall. Mater., Trans.*, 2002.





**MPLUS No.:** MC-01-013

**Title:** Dilatometric Characterization of the Influence of a Standard Heat-Treating Process (the T-6 Temper) on the Dimensional Stability of a Die Cast Aluminum

**User Organization:** Ohio State University  
Columbus, OH 43210



**User Contact:** S. Raman, 614-688-3117  
[raman.13@osu.edu](mailto:raman.13@osu.edu)

**ORNL R&D Staff:** Gerard. M. Ludtka, 865-574-5098  
[ludtkagm1@ornl.gov](mailto:ludtkagm1@ornl.gov)

**Relevance to OIT:** Metalcasting, Aluminum

**Objective:** Performance and design limitations of aluminum die castings depend tremendously on the resultant microstructure and residual stresses that evolve during the initial die casting process and subsequent final heat treatment of these castings. The shrinkage, shape change, distortion, and residual stresses observed in heat-treated die cast aluminum component can be a direct result of thermal cycle. This project utilized the ORNL MPLUS facility's high-speed quenching dilatometer to investigate the influence of a standard solution heat treatment and tempering cycle on the dimensional stability of a die cast aluminum alloy.

**Results:** Aluminum alloy die castings are being utilized for a whole spectrum of applications which include use as automobile engines. One automobile manufacturer plant in Ohio alone makes 4,500 aluminum alloy engines per day. For a specific application, the performance and design limitations depend tremendously on the prior history of the final component which includes the initial casting cycle and subsequent heat treatment process. Both of these steps can result in significant residual stresses that can result in premature failure or reduced life of the final component in service. A major cause for the development of these residual stresses is the dilation strain due to a thermal transient and often involves phase transformation (microstructural) volume changes. These thermal cycles can be intended, such as a heat treatment process to develop the required properties, or the result of the component life cycle such as heating and cooling cycles during use. A standard heat treatment cycle employed for the die cast aluminum alloy A357 (nominally Al-7Si-0.5Mg) is the T6 temper that actually is the combination of the T4 and T5 heat treatments. The initial T4 thermal treatment is a solution heat treatment and quenching operation that typically involves holding the alloy at 540°C for 2 h before quenching in a heated water bath. The subsequent artificial aging heat treatment cycle, given the T5 designation, is performed rather quickly after quenching and involves heating the aluminum alloy to 175°C for 16 h and quenching the part. Rather significant residual stresses can be measured in die

cast aluminum components after these heat treatment cycles and so this endeavor utilized dilatometry to identify the cause of these induced stresses. The die cast aluminum alloy A357 was used as a surrogate in this study for investigating the performance of an A383 type (Al-10.5Si-2.5Cu) aluminum die cast alloy used for engine applications.

The following figure is the dilatometer output of length strain (change in length divided by the initial length) versus temperature for the T4 heat treatment cycle portion of the T6 temper on an A357 die cast aluminum alloy specimen. This demonstrates that a significant final length decrease of -0.56% was measured for this alloy behavior during solution heat treatment. This corresponds to a volume decrease of -1.69% which is on the same magnitude (but opposite sign) of overall dilation strain observed in quenched steels that can develop extremely high levels of residual stress (relative to final yield strength) as determined through x-ray diffraction and neutron diffraction residual stress measurement techniques. Therefore, the shrinkage, shape change, distortion, and residual stresses observed in heat treated die cast aluminum components can be a direct result of this T4 heat treatment cycle used to develop the final properties for the actual component for its intended application.

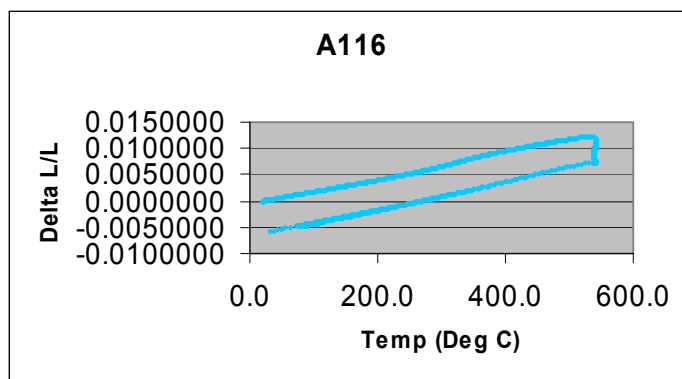


Fig. 1. Dilation strain measured by dilatometry during the T4 heat treatment cycle on an A357 die cast aluminum alloy.

The T5 artificial aging heat treatment cycle was also studied for its contribution to distortion and residual stress. Although not shown here, the dilatometry results show essentially no dilation strain (volume change) associated with any phase transformation or solute segregation (or precipitation reaction) during this part of the T6 temper thermal treatment. It is important to note though that this thermal cycle which involves a rapid quench to ambient temperature indeed can result in residual stress development. This would be the direct result of the temperature gradient during the quenching cycle that could result in sufficient thermal strains as to exceed the yield strength of the material although no phase transformation was observed in the dilatometry output. To clarify this conclusion, we calculated the thermal expansion coefficient for this alloy from the length



strain versus temperature data and obtained a coefficient of thermal expansion of  $25.7 \times 10^{-6} \text{ m/(m}^\circ\text{C)}$ . Using this value and a temperature gradient,  $\Delta T$ , of  $100^\circ\text{C}$ , a strain of 0.26% is calculated which definitely exceeds the standard 0.2% yield strength of the material and very much exceeds the proportional limit, or 0.02% yield strength, of this die cast material. Therefore, this demonstrates that the manner in which a component is cooled from its elevated temperature heat treatment cycle can induce significant residual stresses in the final part although no dilatometry-measured phase transformation or other microstructural change occurs during that thermal transient. If possible, slow cooling should be employed for this T5 part of the T6 temper designation to avoid this source of residual stress development in the final component.

**Reports/Publications/Awards:**

G. M. Ludtka and S. Raman, "Dilatometric Characterization of the Influence of a Standard Heat-Treating Process (the T-6 Temper) on the Dimensional Stability of a Die Cast Aluminum," MPLUS report, December 2002.



**MPLUS No.:** MC-01-014

**Title:** Hardenability of Next-Generation High-Strength Steels for Oil/Natural Gas Transportation Pipelines

**User Organization:** Engineering Mechanics Corporation of Columbus (EMC<sup>2</sup>)  
Columbus, OH 43221

**User Contact:** Zhili Feng, 614-459-3200  
[zfeng@columbus.rr.com](mailto:zfeng@columbus.rr.com)

**ORNL R&D Staff:** Suresh Babu, 865-574-4806  
[babuss@ornl.gov](mailto:babuss@ornl.gov)



Zhili Feng from Engineering Mechanics Corporation of Columbus (EMC<sup>2</sup>)

**Relevance to OIT:** Steel, Chemical, Petrochemical

**Objective:** Solid-state phase transformation and resultant microstructures are critical to the development of next-generation high-strength steels used in pipeline welded constructions. The microstructural heterogeneity in the welded structure is expected to have large influence on the final performance of these welds. In this project, phase transformations and resulting microstructure evolution were evaluated in four steels (see Table 1) using the Gleeble® thermomechanical physical simulator, SEM and other relevant materials characterization facilities of MPLUS.

Table 1: Compositions of steel (wt. %)

ID	C	Mn	Si	Ni	Cu	Cr	Mo	V	Nb	Ti
1	0.06	1.85	0.1	0.13	0.27	0	0.22	0	0.04	-
2	0.04	1.73	0.3	0.27	0.24	0.08	0.27	0.001	0.067	0.018
3	0.06	0.9	0.27	1.67	1.16	0.99	0.4	0.004	0.002	0.002
4	0.06	0.99	0.27	0.75	0.98	0.51	0.5	0.059	0.02	-

**Results:** Four steels (see Table 1) were considered in the research. The steels were subjected to three different peak temperatures (1284, 891, and 741°C) with two (slow and rapid) cooling rates in the Gleeble® thermomechanical simulator. The transformation rates during heating and cooling were measured using a dilatometer. Austenite formation in the steels was found to be complex while heated to a temperature 741°C; (in between Ac<sub>1</sub> and Ac<sub>3</sub> temperatures). The results show continued growth of austenite (Fig. 1a) even while cooling from peak temperature, before the ferrite growth occurs. This phenomenon will modify duplex ferrite + martensite microstructure that may form in the heat affected zone (HAZ). The results show that steel 1 had a high hardenability compared to steels 2 (Fig. 1b). This result indicates the steel 1 has higher probability of forming hard martensite microstructure in the HAZ and weld metal region for a given weld-cooling rate. Conversely, the steel 2

can lead to the formation of tough acicular ferrite/bainitic microstructure for similar cooling rate. Results from other steels are presented in a separate report. All the measured transformation and microstructural characterizations are being used to select optimum steel for pipeline construction that will maximize the tough acicular ferrite/bainitic microstructure in the welds.

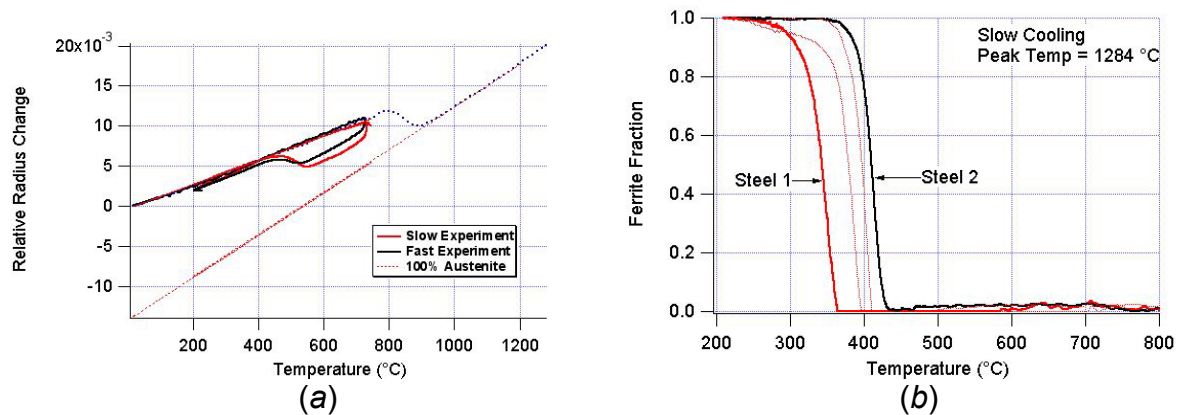


Fig. 1 (a) Typical relative radius change with temperature for a steel while heating to a temperature between the  $A_{c1}$  and  $A_{c3}$  temperatures and (b) measured ferrite fraction formed with temperature for a given cooling rate and a peak temperature for different steels.

### Reports/Publications/Awards:

Z. Feng, "Hardenability of Next-Generation High-Strength Steels for Oil/Natural Gas Transportation Pipelines," MPLUS report, October 2002.

**MPLUS No.:** MC-01-015



**Title:** Statistical Analysis of Time-Series Data  
on Temperature and Resistivity  
Collected from Recovery Boiler Floor  
Tube Membranes

**User Organization:** Mead Central Research  
Chillicothe, OH 45601-3478

**User Contact:** James D. Willis, 740-772-3748  
[jdww3@mead.com](mailto:jdww3@mead.com)

**ORNL R&D Staff:** J. R. Keiser, 865-574-4453  
[keiserjr@ornl.gov](mailto:keiserjr@ornl.gov)

**Relevance to OIT:** Forest Products

**Objective:** The objective of this MPLUS project was to evaluate the use of statistical methods of regression and analysis of variance to time-series data from probes installed in recovery boiler floor tube membranes at Mead-Escanaba.

**Results:** Dennis Wolf and Richard Counts of ORNL's Computer Science and Mathematics Division analyzed data collected from Mead Corporation's paper mill in Escanaba, Michigan, in an effort to try to determine the cause of cracking in floor tube membranes in the mill's recovery boiler. The data included measurements collected by Savcor AB from electrical resistivity probes installed at three locations in the boiler floor and boiler performance data collected by the boiler operators.

The approach to this study involved analysis of two months worth of data collected during a period when selected operating parameters were systematically varied. Statistical analysis techniques were used in an effort to identify the operating parameters that caused high conductivity values that were suggestive of the presence of a molten or partially molten phase very near the surface of the floor membrane.

The analysis process identified four relationships with significant correlations. These are:

1. There was a negative correlation in the resistivity values measured at the sensors on the front of the floor and these on the rear of the floor.
2. There was a positive correlation in the resistivity values measured at the sensors on the floor near the left wall and those on the rear of the floor.
3. High resistivity levels positively correlated with high levels of carbon monoxide and the total reduced sulfur.

4. Resistivity levels tended to increase with increasing oxygen in the combustion gas and with a higher air flow.

Although some correlations were identified in this initial analysis, it was proposed that a more systematic experimental program should be constructed and carried out with the cooperation of Mead and Savcor. In particular, a two phase testing program was suggested. During the first phase, the systematic variation of parameters would be conducted, and the process variables that have the greatest effect on resistivity would be identified. In the second phase, optimal settings would be determined for the parameters identified as being the most critical.

For the first phase of this program, 13 factors or variables would be evaluated. These include: concentration of dissolved solids in the black liquor fed to the boiler, temperature of the liquor being fed to the boiler, production rate of the black liquor, amount of No. 6 fuel oil being co-fired, primary wind box air flow, secondary wind box air flow, tertiary wind box air flow, the sulfidity of the black liquor feed, the size of the nozzle used for feeding the black liquor to the boiler, whether or not the boiler is being operated in a rotofiring mode, the amount of bleed off from the SO<sub>2</sub> scrubber sump, the soot-blown sequence being used, and the wood source (hardwood, softwood or mixed) being processed and producing the black liquor.

It was proposed that a special statistical “screening design” be used to construct a test program that would let the 13 variables be investigated in fewer than 25 runs.

#### **Reports/Publications/Awards:**

D. Wolf and R. Counts, “Recovery Boiler Membrane Cracking Study,” MPLUS report, February 2002.

**MPLUS No.:** MC-01-017

**Title:** Preparation of Spheres (1 to 2 mm diam) of a Magnesium Alloy for Improving Process Efficiency of Thixomolding®

**User Organization:** Thixomat  
Ann Arbor, MI 48108

**User Contact:** D. M. Walukas, 734-995-5550, ext. 234  
[mwalukas@thixomat.com](mailto:mwalukas@thixomat.com)

**ORNL R&D Staff:** V. K. Sikka, 865-574-5112  
[sikkavk@ornl.gov](mailto:sikkavk@ornl.gov)



**Relevance to OIT:** Metalcasting

**Objective:** Thixomolding® of magnesium alloys is a commercially used process for near-net shaping of a large number of components. The process is capable of producing thin sections with thickness of  $< 1$  mm and of significant complexity. The feed stock for the Thixomolding® machines is generally chips, which has an irregular shape and a broad range of sizes. The purpose of this MPLUS project was to evaluate the use of the Uniform Droplet Process for producing 1- to 2-mm-diam spheres of the commercially used magnesium alloy.

**Results:** The Uniform Droplet Process was used to carry out the work scope of this MPLUS project. The process required melting Mg alloy, which is ejected out of nozzles about half the size of the desired particles. For the desired size particles in Thixomolding®, the hole size had to be between 0.5 and 1 mm. The liquid stream is uniformly broken by the use of a Piezo electric device, and the shape of the particles (droplets) is controlled by passing them through an electrically charged plate. While the process had been successfully developed for Sn-, Al-, and Cu-based alloys, the Mg-based alloy posed many issues. The most difficult of them was to prevent the hole at the bottom of the crucible from clogging. Even with inert cover gas, the oxidation of the Mg alloy kept clogging the crucible's opening. After several trials, it was concluded that the uniform droplet process was not feasible for producing uniform size spheres from the Mg alloy of interest for Thixofforming.

#### **Reports/Publications/Awards:**

V. K. Sikka, "Preparation of Spheres of a Magnesium Alloy for Improving Process Efficiency of Thixomolding®," MPLUS report, January 2003.





**MPLUS No.:** MC-01-019

**Title:** Feasibility Study for Hot Extrusion of High Toughness Cemented Carbide Composites

**User Organizations:** Smith International, Inc.  
Houston, TX 77205-0068  
University of Alabama  
Birmingham, AL 35294-4461

**User Contacts:** Zak Fang, 281-233-5869  
[zfang@smith.com](mailto:zfang@smith.com)  
Burton R. Patterson, 205-934-8454  
[bpatters@eng.uab.edu](mailto:bpatters@eng.uab.edu)



From left to right, Burton Patterson from The University of Alabama at Birmingham, Vinod K. Sikka from ORNL, and Zak Fang from Smith International, Inc.

**ORNL R&D Staff:** Vinod Sikka, 865-574-5112  
[sikkavk@ornl.gov](mailto:sikkavk@ornl.gov)

**Relevance to OIT:** Mining, Petrochemical, Powder Metallurgy

**Objective:** The major objective of this user project was to demonstrate: (1) if extrusion process could be used to consolidate double cemented carbide (DC carbide) into long bars of different shapes (rounds, rectangle, and tubular); and (2) if the extrusion consolidated product offers superior properties as compared to hot-pressed product.

The DC carbides are double-composite material, where WC is composited with cobalt. Composited material with each tungsten carbide particle with Co is recomposited in cobalt matrix. Such carbide has the advantage of significantly higher toughness than the conventional WC-Co composites. The DC carbide contains a higher amount of cobalt and tends to have somewhat lower hardness than conventional WC-Co composites. The higher toughness of DC carbides is highly desirable for drilling and high rate machining applications. The purpose of this project was to develop the hot extrusion process for low-cost production of large size pieces of DC carbides.

**Results:** The user project resulted in the following key findings:

1. Extrusion can be used successfully in consolidating WC-Co double cemented carbides into large round and rectangular shapes. Based on this result, it is anticipated that tubular product will not be a problem. It will, however, require a more complex billet (one with a hole for mandrel and inner tube). The extrusion process provides several advantages: (a) simple process, (b) can consolidate large parts, (c) can produce large shaped parts, (d) more dense components produced as opposed to hot pressing, (e) more economical than hot pressing and subsequent

assembly of small parts into finished components, and (f) can result in cutting tools with minimum time lost in change over as opposed to conventional tools possible by hot pressing.

2. Mechanical properties of the DC carbide produced by extrusion product were: (a) directional because of elongation of the matrix phase (Co) in the extrusion direction, and (b) they were better or equal to that for hot-pressed material for toughness properties.

Future plans are to: (1) explore the fabrication of tubular product, and (2) explore testing of extruded DC carbide for certain applications.

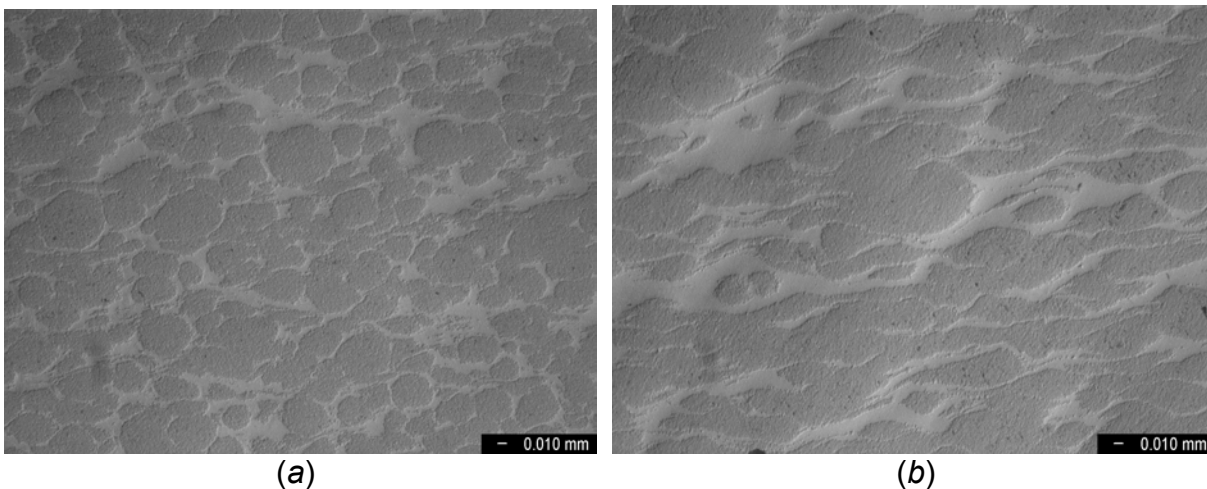


Fig. 1. Microstructure of extruded double cemented carbide: (a) transverse orientation, and (b) longitudinal orientation.

#### **Reports/Publications/Awards:**

V. K. Sikka, B. R. Patterson, and Z. Fang, "Double Cemented Carbide Composite," MPLUS report, 2001.

X. Deng, B.R. Patterson, K.K. Chawla, M.M. Estrada, B.V. Patel, M.C. Koopman, Z. Fang, G. Lockwood, A. Griffo, J. Bitler, and V.K. Sikka, "Double Cemented Carbide Composite," MPIF conference, Orlando, FL, June 2002.

**MPLUS No.:** MC-01-020

**Title:** Select Alloys, Conduct In-Plant Tests, and Characterize Test Coupons of Candidate Hood Materials

**User Organization:** Weirton Steel Corporation  
Weirton, WV 26062-4989

**User Contact:** H. M. Synder, 304-797-4999  
[howard.synder@weirton.com](mailto:howard.synder@weirton.com)

**ORNL R&D Staff:** Vinod Sikka, 865-574-5112  
[sikkavk@ornl.gov](mailto:sikkavk@ornl.gov)

**Relevance to OIT:** Steel, Welding, Process Heating

**Objective:** Hoods on basic oxygen furnaces are used for various reasons including heat recovery. However, current materials often have corrosion wear and cost issues. The purpose of this MPLUS project was to select and prepare corrosion-resistant materials into test coupons that would be subjected to in-plant testing on BOF hoods, then, evaluated and characterized to assess the relative performance of these candidate materials under in-plant conditions.

**Results:** This project dealt with fabrication of tubular test panels of candidate materials and weld overlays for installation in BOF hoods at Weirton Steel. The starting base panels of carbon steel tubes were supplied by Weirton Steel. Candidate materials used for panel fabrication included: (1) Alloy 622 weld overlay, (2) Alloy 625 weld overlay, (3) Al-clad weld overlay, (4) IC-221LA weld overlay, and (5) Fe-3Cr-3W(V) monolithic tube. The weld overlays of alloys 622 and 625 were prepared using aluminum wire, which resulted in surface aluminum composition of approximately 10 wt %. IC-221LA is a weld wire composition for nickel aluminides and was produced as an experimental batch at Stooddy Company. The Fe-3Cr-3W(V) is a new patented alloy developed at ORNL. The alloy composition was melted, cast into ingots, and extruded into tubes. The tube's outside and inside diameters were machined slightly to produce smooth surfaces. A total of four panels with detailed mechanical and physical property data were supplied to Weirton Steel. Figure 1 shows a panel that was installed in a BOF hood at Weirton. The specimens are still under test.

The chemical analysis of the base carbon steel, various weld overlays, and 33VT alloy are presented in Table 1. Note that these alloys vary in composition from nickel-base to iron-aluminide base to high-strength Fe-3Cr-3W steels.





Fig. 1. Photograph of one of the panels fabricated for installation in a BOF hood at Weirton Steel.

Table 1. Chemical compositions of candidate materials

Element	Steel AISI Grade 55	Alloy 625	Alloy 622	IC-221LA	Aluminum Clad	33VT
Ni	-	58.0	56.35	81.1	-	-
Cr	-	20.0-23.0	20.5	7.7	-	2.94
Mo	-	8.0-10.0	14.2	1.43	-	-
Fe	98.665	5.0 max	2.3	-	90-92	93.114
Mn	0.85/1.20	0.5 max	0.5 max	-	-	0.5
Co	-	1.0 max	2.5 max	-	-	-
Nb	-	3.15-4.15	-	-	-	-
V	-	-	0.35 max	-	-	0.25
W	-	-	3.2	-	-	2.85
Ta	-	-	-	-	-	0.1
Zr	-	-	-	1.7	-	-
C	0.26 max	0.1 max	0.015 max	-	-	0.097
N	-	-	-	-	-	-
P	0.035 max	0.015 max	0.02 max	-	-	0.005
Al	-	0.4 max	-	8.0	8-10	-
B	-	-	-	0.008	-	-
Si	0.15/0.3	0.5 max	0.08 max	-	-	0.14
S	0.04 max	0.015 max	0.02 max	-	-	0.004
Ti	-	0.4 max	-	-	-	-

### Reports/Publications/Awards:

M. L. Santella, J. D. McNabb, and V. K. Sikka, "Tube Panel Fabrication for Installation in BOF Hoods at Weirton Steel," MPLUS report, 2001.

**MPLUS No.:** MC-01-021

**Title:** The Effect of Boron and Zirconium on the Resistance of HAYNES® 214™ Alloy to Strain Age Cracking

**User Organization:** Haynes International Inc.  
Kokomo, IN 46904-9013

**User Contact:** Mark D. Rowe, 765-456-6228  
[mrowe@haynesintl.com](mailto:mrowe@haynesintl.com)

**ORNL R&D Staff:** Suresh Babu, 865-574-4806  
[babuss@ornl.gov](mailto:babuss@ornl.gov)



Mark Rowe from  
Haynes International Inc.

**Relevance to OIT:** Chemical, Combined Heat and Power

**Objective:** Alloy 214 is being considered for use in low stress, high-temperatures (~900 °C) and oxidizing environment, therefore its high temperature ductility is an important design criterion. It is speculated the precipitation and dissolution of gamma prime during heating and cooling and presence of boron and zirconium in the alloy may alter the high temperature ductility. The objective of this MPLUS project was to measure the ductility of Alloy 214 while it was being heated through the gamma prime precipitation temperature range, and compare it to modified Alloy 214 without boron and zirconium additions. This was followed up with microstructural characterization.

**Results:** Two alloys were studied in this MPLUS research. One alloy (EN1001) was made with intentional additions of boron and zirconium, similar to commercial HAYNES® 214™ alloy, while the other alloy (EN1101) was made without boron or zirconium. The specimen was heated to 1100°F at a conveniently rapid rate, held for ten seconds, then heated at a linear rate to the test temperature, and pulled to failure at a 0.063 in. per minute stroke rate, while maintaining the test temperature. The alloy with boron and zirconium addition displayed significantly greater ductility in the Gleeble test than the alloy without boron and zirconium, as shown in Figure 1.

The MPLUS research program comparing the elevated temperature ductility of Alloy 214 with and without boron and zirconium additions provided several useful results. Prior work was confirmed regarding the effectiveness of boron and zirconium additions at improving intermediate temperature ductility. A Gleeble test method was shown to be effective for evaluating intermediate temperature ductility in gamma prime strengthened alloys. Follow-up Gleeble testing and microstructural characterization is underway at Haynes. An additional MPLUS program was initiated to complement the previous work with microstructural characterization in an effort to explain the role of boron and zirconium. A technical presentation based on the MPLUS work and work at Haynes is planned for the 2003 American Welding Society national conference.

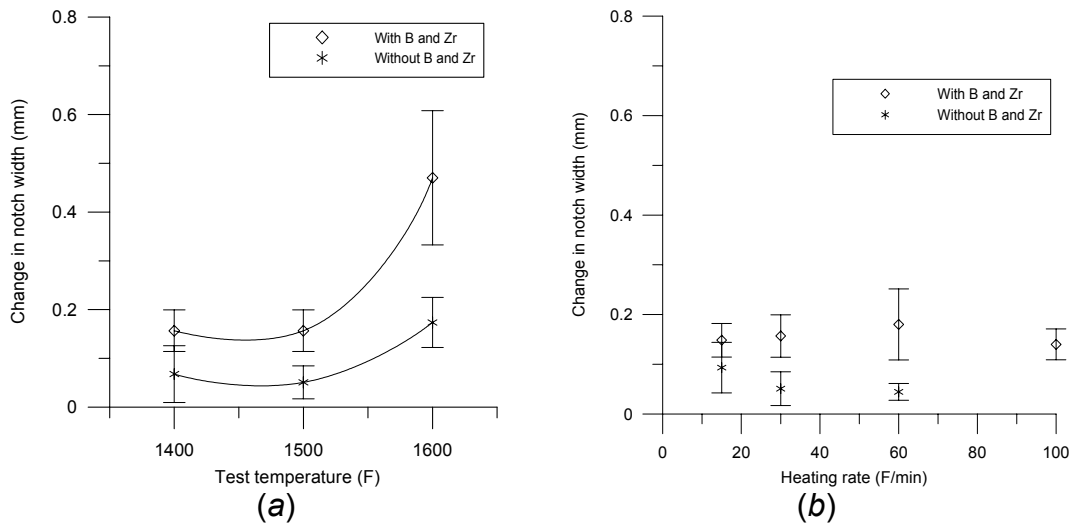


Fig. 1: (a) Gleeble test results; ductility at the notch tip prior to crack initiation and change in notch width, as a function of the test temp. (b) Gleeble test results; ductility at the notch tip prior to crack initiation and change in notch width as a function of the heating rate from 1100 to 1500°F.

#### Reports/Publications/Awards:

M. D. Rowe, "Gleeble Testing of HAYNES® 214™ Type Alloys under the MPLUS Program," MPLUS report, January 2001.



**MPLUS No.:** MC-01-022

**Title:** Detection of Plant Cell Dimensions in Loblolly Pine Wood using Micro-CAT Scan Techniques

**User Organization:** Weyerhaeuser Company  
Federal Way, WA 98003

**User Contact:** N. C. Wheeler, 360-278-3535  
[nick.wheeler@weyerhaeuser.com](mailto:nick.wheeler@weyerhaeuser.com)

**ORNL R&D Staff:** M. J. Paulus, 865-241-4802  
[paulusmj@ornl.gov](mailto:paulusmj@ornl.gov)



Nick Wheeler from  
Weyerhaeuser Company

**Relevance to OIT:** Forest Products

**Objective:** The objective of this MPLUS project was to determine the ability of micro-CAT scan to detect differences in cell wall thickness and cell lumen diameter among standardized samples as a means of predicting final product value.

**Results:** Micro-computed tomography (micro CAT) is a high-resolution X-ray imaging tool that has the potential to be used to measure wood cell anatomy. Unlike traditional assays that require the destruction of the sample or more recently developed surface scanning technologies, micro CAT uses penetrating radiation to build a 2D or 3D map of the internal, non-disturbed structure of the sample. Figure 1 shows the transition between alternate year's late wood on the right and early wood on the left. In addition, two resin canals are present in the latewood. A single ray parenchyma is adjacent to the lower resin canal. There is variation among adjacent daughter cells in cell diameter, such that some cell lines consistently produce large diameter cells while other cell lines produce small diameter cells. This variation among cell lines appears to be preserved across annual growth rings.

A subsample of 14 annual rings has been studied to date. For each annual ring, the micro CAT-measured cell diameters in both the radial and tangential directions were compared with the cell diameter value determined by Weyerhaeuser. Micro CAT-measured cell wall thickness was compared with cell wall thickness data also provided by Weyerhaeuser.

In general, the micro CAT cell diameter data agreed very well with the Weyerhaeuser data (Figures 2 and 3). Trends in cell diameter with age were as expected, increasing slightly with time. The correlation coefficient between the two measures was higher for radial diameters than that for tangential diameters ( $r = 0.77$  vs.  $r = 0.46$ , respectively). The overall standard errors were lower for the micro CAT values than the standard errors for the Weyerhaeuser data in the radial direction but were higher in the tangential direction (1.06 vs. 1.12 in the radial direction and 0.71 vs. 0.32 in the tangential direction). Though the correspondence between the two alternate measures

of annual mean cell diameter was very good, the lower standard error estimates in the tangential direction in the Weyerhaeuser data set is difficult to explain. That is, when examining the actual images of tangential cell diameter across each of the measure yearly increments there is large variation among neighboring cell lines in apparently inherent cell diameter (Figure 1). This variation is captured in the micro CAT measurements but is apparently missing in the Weyerhaeuser dataset. Large differences between the cell diameter values in the tangential direction between the micro CAT measurements and the Weyerhaeuser estimates for ages 10 and 14 are apparent. Multiple, repeated measures using the micro CAT image files did not resolve this difference; that is, similar values were obtained with each repeated measure. There are two possible explanations for these differences. First, though every effort was taken to ensure that similar regions within the increment core were measured in both datasets, the micro CAT and Weyerhaeuser values may have come from alternate populations of cells, thus yielding contrasting estimates. And secondly, one of the two estimates may be wrong, but with only a single data point for each, it is not possible to determine if this is the case or which value may be in error.

The correspondence between the micro CAT and Weyerhaeuser estimates for mean annual cell wall thickness was very good ( $r = 0.87$ ). The trend over time towards thicker cell wall was apparent in both datasets (Figure 4). It was not possible to estimate standard errors for the micro CAT annual means because cell wall thickness was estimated on an area basis in each annual increment. That is, information from all cell within a particular scanned increment were used to estimate cell wall thickness.

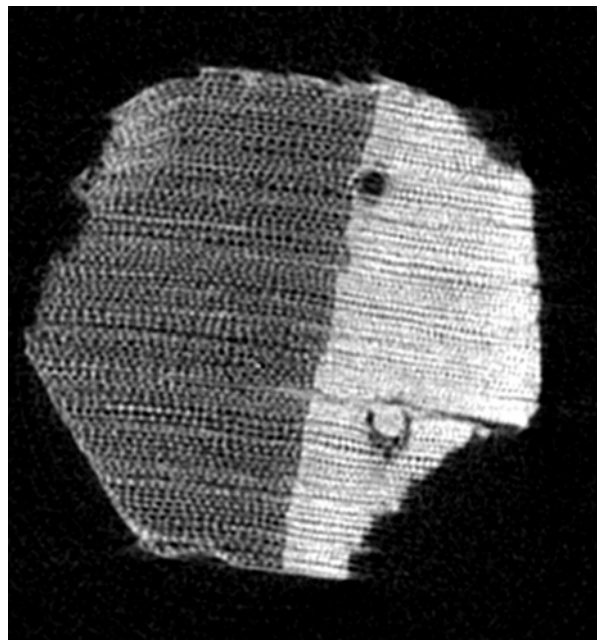


Fig. 1. Tomographic image of a loblolly pine sample showing the inter-year transition between the previous year's late wood (on the right) and the following year's early wood (on the left).



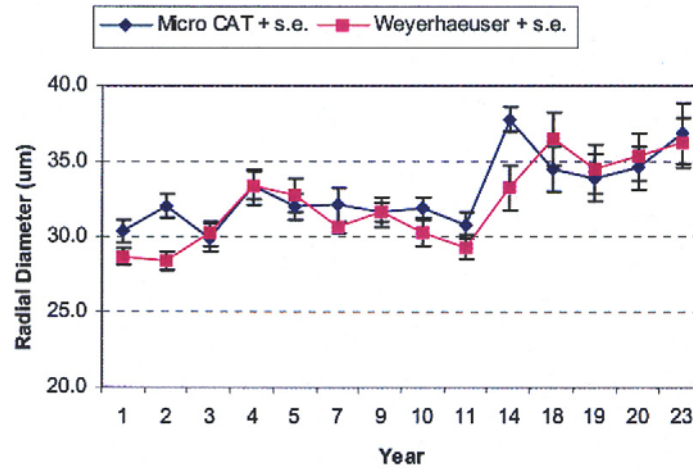


Fig. 2. Comparison of micro CAT and Weyerhaeuser-provided values for cell diameter in the radial direction for loblolly pine across 14 measurement dates/ages.

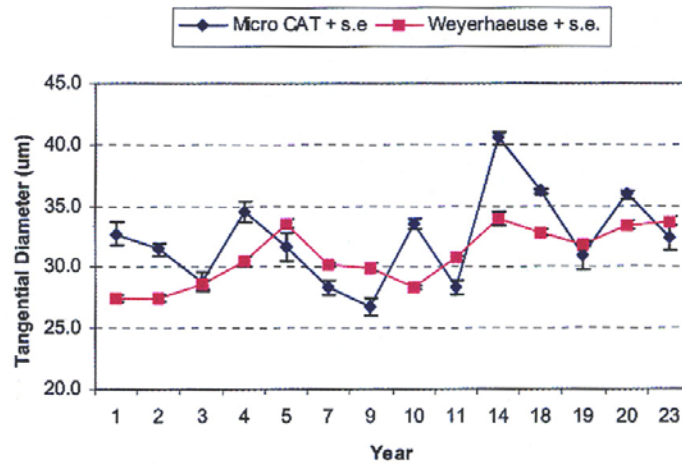


Fig. 3. Comparison of micro CAT and Weyerhaeuser-provided values for cell diameter in the tangential direction for loblolly pine across 14 measurement dates/ages.

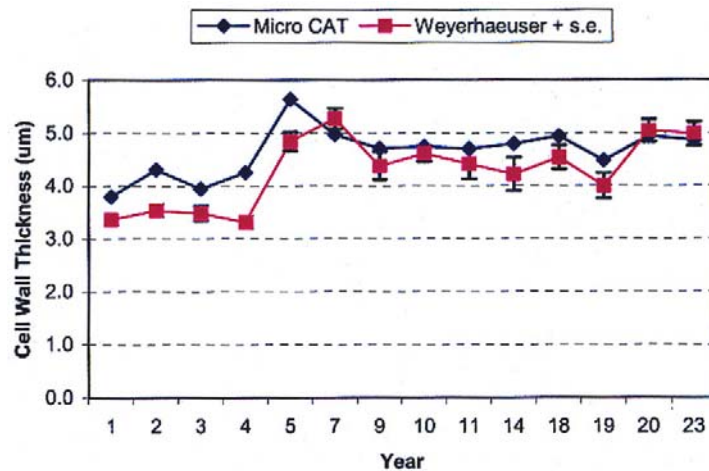


Fig. 4. Comparison of micro CAT and Weyerhaeuser-provided values for cell wall thickness for loblolly pine across 14 measurement dates/ages.

#### Reports/Publications/Awards:

M. J. Paulus and N. C. Wheeler, "Detection of Plant Cell Dimensions in Loblolly Pine Wood using Micro-CAT Scan Techniques," MPLUS report, December 2002.

**MPLUS No.:** MC-01-023

**Title:** Determination of True Stress-Strain Curves of Steels at Elevated Temperatures

**User Organization:** Caterpillar Inc.  
Peoria, IL 61656

**User Contact:** Zhishang Yang, (309) 578-2761  
[YANG\\_ZHISHANG@cat.com](mailto:YANG_ZHISHANG@cat.com)

**ORNL R&D Staff:** Suresh Babu, 865-574-4806  
[babuss@ornl.gov](mailto:babuss@ornl.gov)

**Relevance to OIT:** Mining, Steel, Welding

**Objective:** The objective of this MPLUS project was to determine the true stress-strain curves of steels at elevated temperatures. The obtained data will be used for modeling material processing (welding, rolling, thermal cutting, and heat treatment) in order to optimize material processing parameters for desired residual stress status or distortion control.

**Results:** Three high strength low alloy steels were subjected to tensile testing at different temperatures. The specimen were heated to 1200°C and held for five minutes for homogenization. After that, the specimens were cooled at the rate of 20°C/s to the test temperature. The stress-strain curves will be tested at specified temperatures with the strain rate of  $5.0 \times 10^{-2} \text{ s}^{-1}$ . Typical stress strain characteristics attained at 800°C and 500°C are compared in Figs. 1(a) and (b). The plots show small differences between the steels at 800°C, due to the presence of single-phase austenite. However, at 500°C, the steels show large differences in stress-strain characteristics. This is related to different microstructure that evolves from austenite while cooling at 20°C/s in these steels. This data is of great value to simulation of residual stress development during welding of structural steels used in earthmoving industries.



Zhishang Yang from Caterpillar Inc.

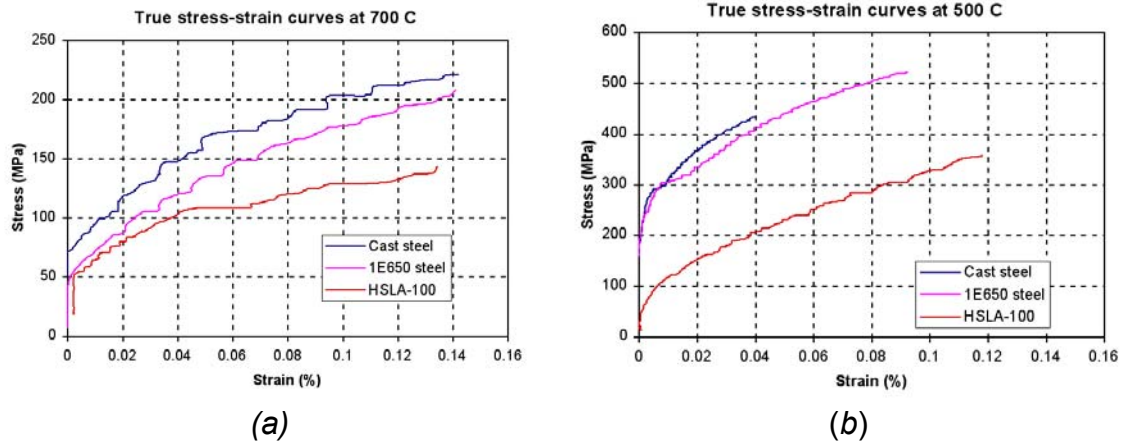


Fig. 1. Comparison of stress strain characteristics attained at (a) 800°C and (b) 500°C for three steels.

### Reports/Publications/Awards:

Zhishang Yang and Suresh Babu, "Determination of True Stress-Strain Curves of Steels at Elevated Temperatures," MPLUS report, February 2002.

**MPLUS No.:** MC-01-024

**Title:** Forming of Thick Section Material using The Vortek Water Stabilized Plasma Lamp

**User Organization:** Native American Technologies Co. Golden, CO 80401

**User Contact:** Jerry Jones, 303-279-7942, ext. 20  
[jonesje1@aol.com](mailto:jonesje1@aol.com)

**ORNL R&D Staff:** Gail Ludtka, 865-576-4652  
[ludtkagm@ornl.gov](mailto:ludtkagm@ornl.gov)

**Relevance to OIT:** Steel, Heat Treating

**Objective:** The purpose of the MPLUS project was to establish the feasibility of utilizing the high density infrared (HDI) technology to thermally form large scale steel components. Some of the advantages of this process would be more efficient and faster rates than achieved by other heating sources.

**Results:** A three-part set of experiments was conducted to establish the feasibility of utilizing the HDI technology to thermally form large - scale components. The initial set of experiments focused on thermally forming 12- by 3-in. plates under stationary processing conditions, and helped establish a more well-defined set of experimental parameters for the second phase of experimental trials. Based on these latter results, a final set of experiments was conducted that established the feasibility for applying the HDI technology to large diameter tubes.

The experimental set-up and robot used to manipulate the Vortek HDI lamp during these trials are shown in Figure 1. The second set of experiments incorporated a rapid thermal forging approach, in which the HDI lamp traveled at a maximum speed, and relied on plate self-quenching to yield good thermal forming characteristics. Table 1 lists the experimental results obtained in this second set of experiments.

A limited number of experiments indicated that the maximum tube deflection was obtained with the HDI processing parameters of 15 mm/s and 900 A. More studies are needed to optimize rapid forming for large diameter tubes.



From left to right, David Harper from ORNL, Jerry Jones from Native American Technologies Company, and Gail Ludtka from ORNL.

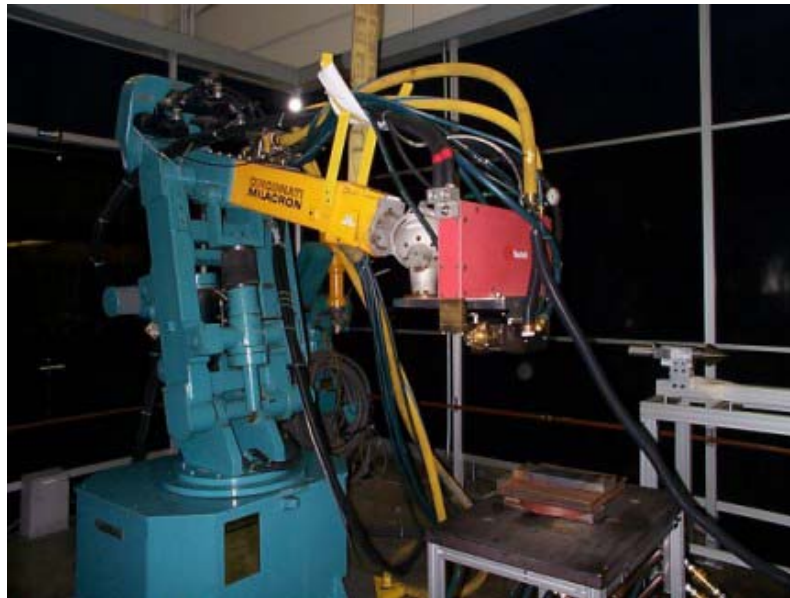


Fig. 1. Cincinnati Milacron robot integrated with the 300-kW Vortek lamp.

Table 1. Second set of experiments with the Vortek lamp based on moving a set travel speed

Reflector = 11.5 cm Water Window installed Plate Size: 12" x 3"					
Sample #	Travel Speed (mm/sec)	Amps	Passe s	Quenche d	Plate Thickness
S-7	10	900	1	1/2	3/8"
S-8	8	900	1	1/2	3/8"
S-9	6	900	1	Yes	3/8"
S-10	5	900	1	Yes	3/8"
S-11	5	1000	1	Yes	3/8"
S-12	5	950	1	Yes	3/8"
S-13	5	1000	1	Yes	1"
S-14	5	900	4	Yes	1"
S-15	5	950	1	Yes	3/8"
S-16	5	950	1	Yes	3/8"
S-17	5	950	1	Yes	3/8"
S-17a	5	950	1	Yes	3/8"
S-18	5	900	6	Yes	1"

Conclusions: The significant results from this project are:

1. It has been demonstrated that using the HDI process, deflections can be obtained in both 3/8- and 1-in.-thick steel plates with the Vortek Lamp system.
2. The results achieved represent significantly faster production rates than what have been achieved with other heat sources.

Also, given that the forming with the Vortek lamp did not include the application of dynamic cooling, the thermal forming times will be even less once the process with the Vortek lamp can be optimized.

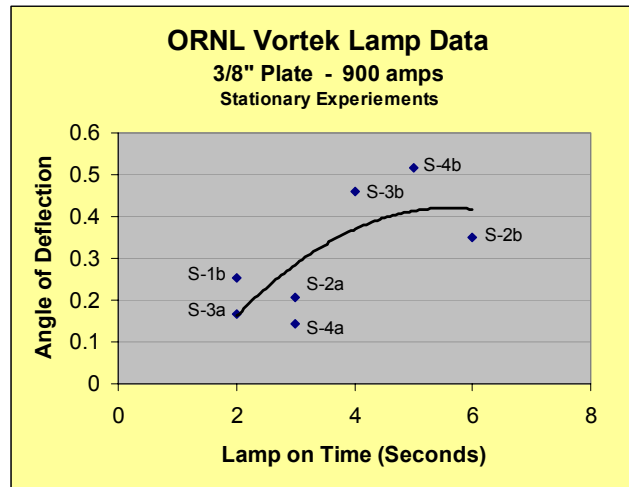


Fig. 2. Thermal forming results generated from the 3.8-in.-thick plate in the first set of experiments (900 A only).

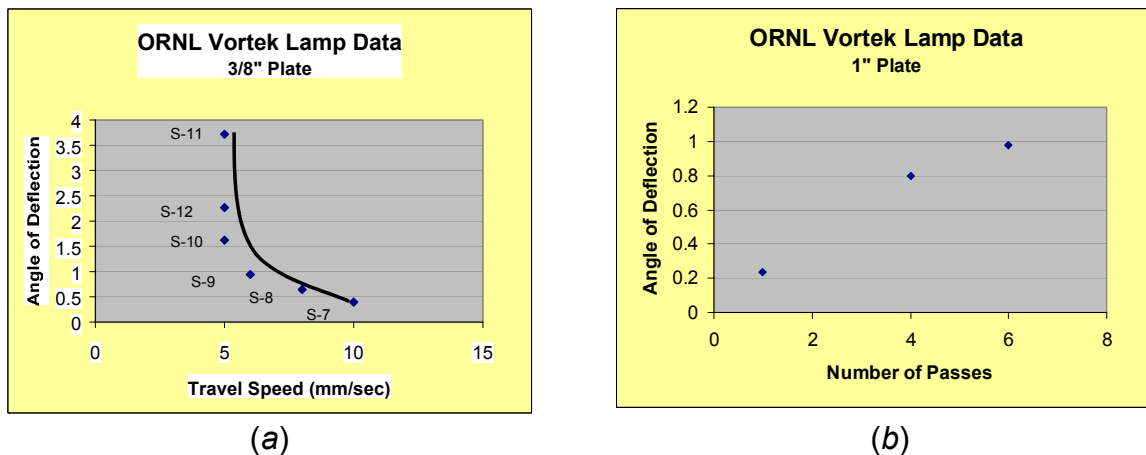


Fig. 3. The second set of experiments indicated that (a) an increasing deflection with decrease in travel speed, and (b) the plate continues to form even after six passes.



Fig. 4. Photograph of HDI tube formed with three forming experiments.

**Reports/Publications/Awards:**

J. Jones, M. M. Mossman, Ludtka, G. M. and Craig Blue, "Thermal Forming using the Vortek Lamp," MPLUS report, August 2001.



**MPLUS No.:** MC-01-025

**Title:** Residual Stress Determination in Friction  
Stir Welded 2024-T3 Aluminum

**User Organization:** University of South Carolina  
Columbia, SC 29208

**User Contact:** M. A. Sutton, 803-777-7158  
[sutton@sc.edu](mailto:sutton@sc.edu)

**ORNL R&D Staff:** C. R. Hubbard, 865-574-4472  
[hubbardcr@ornl.gov](mailto:hubbardcr@ornl.gov)

**Relevance to OIT:** Welding, Aluminum

**Objective:** The purpose of this MPLUS project was to determine how the residual stresses in 6.25-mm-thick 2024-T3 aluminum specimens vary with changes in friction stir welding parameters, a recently developed joining method that has the potential to replace resistance welds in some structural applications. To the best of our knowledge, this research effort is the first time that a combined mixed-mode fracture residual stress measurement study had been performed on FSW joints. As such, the combination of residual stress measurements and the mixed mode fracture experiments formed part of the technical basis for determining the feasibility of using FSW joints to replace riveting or other joining methods in aerospace structures. The data from this experimental program provided baseline information to characterize: (1) the effects of processing parameters on residual stresses, (2) fracture behavior of FSW joints under mixed mode loading conditions that are similar to those observed for flaws in lap splice joints within aircraft, (3) the effect of crack orientation relative to the FSW joint on fracture behavior, and (4) the level of residual stress in the joint prior to fatigue crack growth and stable tearing. Though primary focus was on the effect of residual stress measurements on mixed mode tearing behavior, the effect of these stresses on mixed mode fatigue behavior was also investigated as part of the overall research program.

**Results:** Triaxial Residual Stress about a Friction Stir Weld Measured by Neutron Methods. The friction stir weld (FSW) method holds great promise for joining plates, bars and extrusions of many alloys including industrial- and transportation-related aluminum alloys. In this project researchers from the University of South Carolina are developing a model to predict the microstructure and residual stresses resulting from FSW joining Al 2024-T3 plates. In the first phase of measurements at HFIR detailed residual stress mapping of strains were made in three mutually perpendicular directions (longitudinal, transverse, and normal) to the direction of the FSW weld line. However, recent fracture studies and models of the FSW process indicated the possibility that the stress tensor's principle axes were not along these three primary directions. To



investigate this hypothesis the specimen was taken to the NRU reactor in Chalk River Canada for measurements as HFIR is out of service for upgrades.

To study the orientation of the strain tensor calls for strain measurements in at least ten directions in order to accurately define the direction of the principal axes. A limited number of measurements of the strain tensor were made near the interface between the stir zone and the base metal. Three processing conditions were examined in which the tool rotation speed, tool pressure and tool velocity along the weld were varied. Temperature rise due to the rate of working varied from cold, warm and hot. In consideration that the metal within the stir zone is subject to mechanical shearing, it was surprising to find that the principal axis directions were parallel to the directions assumed in the HFIR experiments and the same directions found in conventional arc welding welds. However, the principal axes were found rotate by as much as  $45^\circ$  about the plate normal axis in the base metal. This probably reflects the material response in providing the mechanical constraint during the stir welding process. The most reasonable explanation for these results is that there is enough heat generated within the stir zone to provide some form of stress relief. The system of stresses associated with thermal expansion and shrinkage in all welds appears to be the principle factor determining the residual stresses in the stir zone.

These neutron residual stress tensor results are the first of their kind in FSW characterization and represent a powerful method of testing and validating residual stress calculations being made at the University of South Carolina. It is expected that the friction-stir methods can be optimized in this and other materials through the use of computation and neutron residual stress measurement.

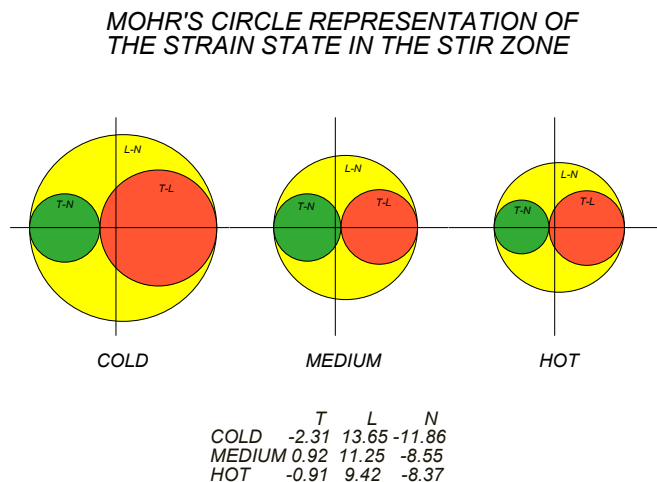


Fig. 1. The strain state within the stir zone represented by a Mohr's Circle construction. The intersections of the circles with the horizontal line give the principal axis strains along the transverse (to the weld line), longitudinal (along the weld line), and normal or perpendicular (to the plate) directions. The vertical extreme in each of the circles gives the shear strain. It is apparent that the strains are largest for the cold stirring process and decrease as the process becomes hot.

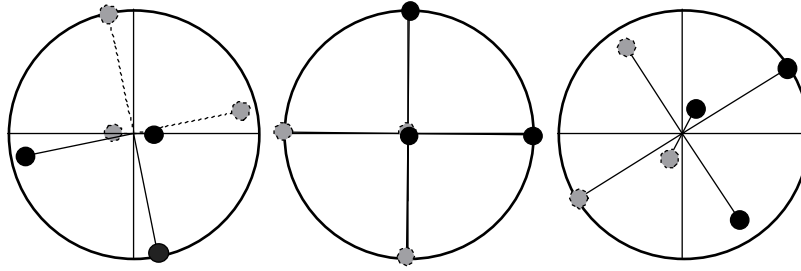


Fig. 2. The directions of the principal axes in base metal on the tool advancing side(*left*), the stir zone (*middle*), and the base metal (*right*) on the tool retreating side represented in stereogram plots. The dark circles are above the "equator" of the stereogram, and the gray circles are below. Note that the principal axes for the stir zone are simply related to the orthogonal axes of the weld geometry. The principal axes for the material just outside the stir zone are rotated away from the stir zone principal axes.

The effect of processing can be summarized as follows. Principal axis rotation is moderate (10 to 30°) and nearly the same on the two sides of the weld in the cold process. In the medium process the rotation is 45° on one side and negligible on the other side. Very little rotation is seen on either side in the hot process. The magnitude of strains is always higher in the stir zone with the largest strains found in the cold process and with moderate decrease in the warm and hot processes. The largest *base metal* strains are seen on one side of the weld in the hot process. We anticipate being able to compare these observations with model calculations that are being developed at the University of South Carolina.

X-ray surface stress measurements are also desired and an assessment of the potential of successful measurements and an experimental plan has been developed. Unfortunately, the grain size of the available specimens prevents good measurements and new specimens will have to be prepared if this approach is to be successful.

### Reports/Publications/Awards:

M. Sutton, C. R. Hubbard, D. Q. Wang, and S. Spooner, "Neutron Diffraction Strain Tensor Measurements in Aluminum Friction-Stir Welds," University of South Carolina, MPLUS report, 2001.



**MPLUS No.:** MC-01-026

**Title:** Soldering/Brazing for Automotive Aluminum Panels using Arc Lamp as a Heating Method

**User Organization:** Ford Motor Company  
Dearborn, MI 48124

**User Contact:** Tsung-Yu Pan, 313-322-6845  
[tpan@ford.com](mailto:tpan@ford.com)

**ORNL R&D Staff:** Mike Santella, 865-574-4805  
[santellaml@ornl.gov](mailto:santellaml@ornl.gov)



From left to right, Mike Santella, Robbie Reed, and David Harper from ORNL, Larry LePrevost from Johnson Manufacturing Co., and Tsung-Yu Pan from Ford Motor Company.

**Relevance to OIT:** Welding, Aluminum

**Objective:** The objective of this MPLUS project was to investigate the possibility of using high-intensity infrared heating techniques for industrial soldering/brazing process on aluminum substrates.

**Results:** A new pulse brazing approach was developed for high production brazing of large structures. In this technique, a plasma lamp technology was utilized to pulse high power density radiant, light, to a predetermined area to simultaneously heat a base aluminum alloy sheet and braze filler metal/flux materials. The lamp was typically pulsed for 2 to 10 s over an area of 2 by 11 cm with power density on the order of 150 to 300 W/cm<sup>2</sup>. The area of heating was readily altered by movement of the lamp by a robotic manipulator. Areas as large as 5 by 35 cm were pulse heated to braze temperatures in seconds. The ability of the technique to heat large areas rapidly allows for heat transfer into the base material which is necessary to allow for fluxing action and wetting and flow of the braze filler metal. This technology could be enabling where brazing of a large structure is necessary without completely enclosing the structure and where welding and torch brazing are not possible or undesirable.

Two types of brazing filler metals were used to make similar joints. In one case a solid wire was used. In the second case, the filler metal wire had a flux core. The brazing characteristics and results were similar for both types of filler metal wires. In both cases, the braze filler metal flowed completely through the joint gaps from the face sides to the root sides. The flow of filler metal completely through the joint gap was evidence that the temperature of the aluminum sheets in the vicinity of the joint was uniform. This temperature uniformity was achieved in 2 to 10 s which is much quicker than would be possible by conventional heating techniques such as torch brazing.

The microstructures of these joints were examined, and they are identical to those achieved with more conventional heating processes. The microstructures of the joints made with Zn-20Al wt % filler metal consisted of aluminum-rich primary dendrites and an interdendritic constituent of aluminum-zinc eutectic. The joints contain some porosity, but the amount and distribution is typical of brazing with fluxes at atmospheric pressure.



Fig. 1. Detail views of the face sides (left) and the root sides (right) of pulsed plasma infrared-heated aluminum braze joints. Joint on the left was made with flux-cored filler metal wire. Joint on the right was made with solid filler metal wire.

### **Reports/Publications/Awards:**

An invention disclosure entitled, "Infrared Brazing of Aluminum Alloys," was prepared and is being pursued. Inventors include staff from ORNL, Ford Motor Company, and Johnson Manufacturing Company.



**MPLUS No.:** MC-01-028

**Title:** Rapid Infrared Preheating of Extrusion Die

**User Organization:** Alcoa Engineered Products  
Spanish Fork, UT 84660

**User Contact:** D. Mark Shelley, 801-798-8730,  
[mark.shelley@alcoa.com](mailto:mark.shelley@alcoa.com)

**ORNL R&D Staff:** Craig A. Blue, 865-574-4351  
[blueca@ornl.gov](mailto:blueca@ornl.gov)



Mark Shelley from  
Alcoa Engineered Products

**Relevance to OIT:** Aluminum, Forging

**Objective:** Extrusion dies and die-tooling sizes range from 11.875 in. by 1 to 24 in. by 11 in. (thickness/diameter). In order to have these dies heated to the extrusion temperature of 820°F, these dies have to be soaked in convection type furnaces for approximately 4 h. Therefore, real time changes in die tooling is not possible, a predetermined extrusion schedule must be developed to allow for the proper heating time on the tooling. Variations in the extrusion schedule can cause large down time of the presses if the tooling is not preheated to the proper temperatures. This MPLUS work focused on the rapid preheating of the extrusion dies in an effort to accomplish real time changes in extrusion dies without maintaining large numbers of dies at the extrusion temperature. This would result in large energy savings, reduction in extrusion press downtime, improved product dimensional control, and potentially extension of die life. The areas investigated included rapid preheating of the tooling and its effects on die dimensionality as well as one side heating versus two sided heating. The two-sided heating would be modeled at ORNL due to the unavailability of a two-sided, large infrared furnace, which was required in order to accomplish this work.

**Results:** An 88-kW, 24- by 24-in. flat bed infrared furnace was utilized for the experimental work at ORNL. Two separate dies provided by Alcoa Engineered Products were heated in a 88-kW, single sided infrared heating unit at ORNL (Figure 1).

**Die Material H-13:** -1 in. thick by 18 in. diam.  
-2 in. thick by 18 in. diam.

**Infrared System:** -88 kW, single sided, infrared drop-bottom batch furnace.  
-Three power levels utilized (70, 80, and 90%).

The infrared heating was able to preheat a 1- by 12-in. die to an operating temperature of 820°F in 8 min at 70% power.



Fig. 1. ORNL in-house 88-kW furnace heating dies during an experimental run.

Due to the unavailability of a double sided heater, modeling was utilized in an effort to extract the potential heating times for a double sided infrared furnace (see Figure 2).

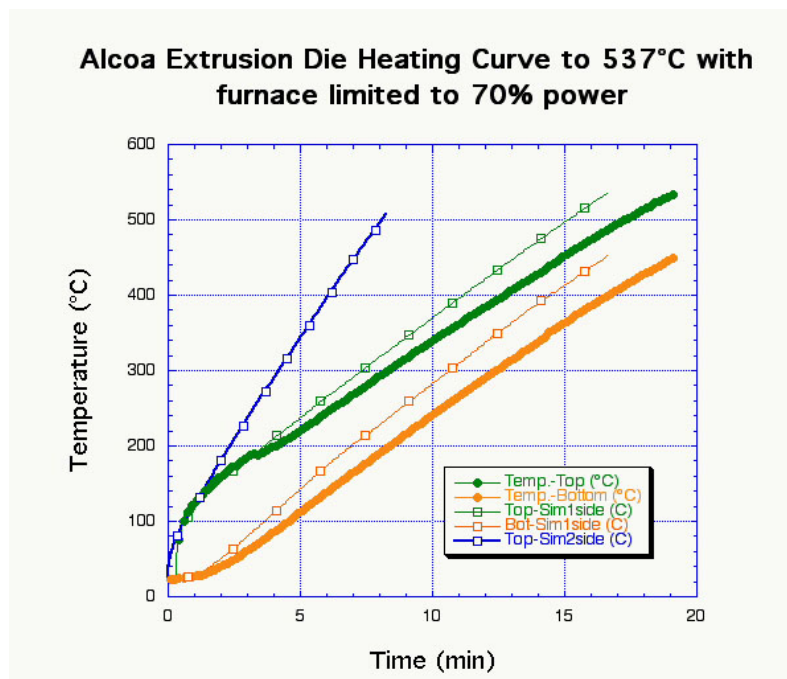


Fig. 2. Modeling results agree well with experimental results for one sided heating. Shown is front and back side temperature readings on a die, experimental vs. modeled. The blue line depicts two-sided infrared heating showing that a 2-in.-thick by 19-in.-diam tool could be heated to temperature in 8 min at 70% power.



Modeling was also accomplished for the largest thickness dies of 10 in. (see Figure 3).

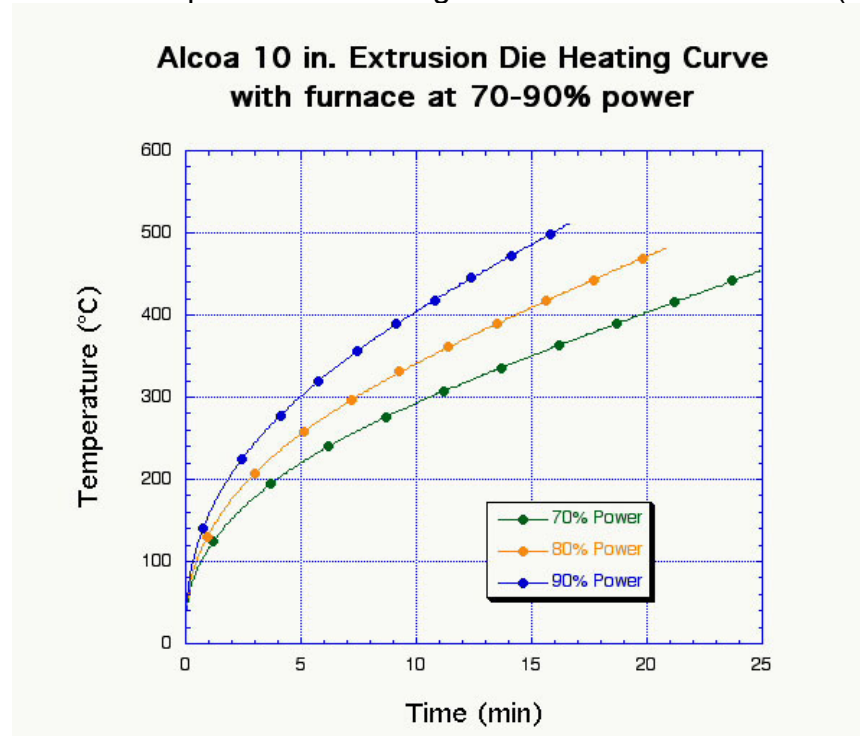


Fig. 3. Two sided heating model reveals that a 10- by 18-in. die can be heated to operating temperature in less than 30 min.

Conclusions: Infrared heating can provides real time heating of dies for tool changing in an aluminum extrusion facility.

Infrared Single Sided Heating: -Preheats 1- by 18-in. dies to 820°F in 3.5 min.  
-Preheats 2- by 18-in. dies to 820°F in 8 min.  
-Experimental and modeling heating results match well.

Infrared Double Sided Heating Model: -Preheat 10- by 18-in. dies to 820°F in less than the time needed for tooling change.  
-Initial prototype design capable of heating entire die stack in less than 30 min completed.

#### Reports/Publications/Awards:

M. Shelley, B. Mansure, C. A. Blue, S. Viswanathan, and P. Angelini, "Rapid Infrared Preheating of Extrusion Die," MPLUS report, 2001.



**MPLUS No.:** MC-01-029

**Title:** Fabrication, Heat-Treating Microstructures, and Tensile Testing of a High-strength 3Cr-3W-V(Ta) Alloy Plate

**User Organization:** Nooter Consulting Services  
St. Louis, MO 63104

**User Contact:** Maan H. Jawad, 314-421-7339  
[mhjawad@nooter.com](mailto:mhjawad@nooter.com)

**ORNL R&D Staff:** V. K. Sikka, 865-574-5112  
[sikkavk@ornl.gov](mailto:sikkavk@ornl.gov)



Maan H. Jawad from  
Nooter Consulting Services

**Relevance to OIT:** Chemical, Steel, Petrochemical, Welding, Process Heating

**Objective:** A 3Cr-3W-V(Ta) alloy composition was developed that has the potential of not only doubling the strength of the standard 2.25Cr-1Mo steel but also potentially can be used in the welded structure with the post-weld heat treatment. The purpose of this MPLUS project was to fabricate one to two plates of the subject alloy, heat treat it to the optimum microstructure, and supply to Nooter for welding trials with and without the post-weld heat treatment. Favorable results of such trials will open up many potential applications as a structural material for large chemical reactor vessels and tubes.

**Results:** Two Fe-3Cr-3W(V) alloys with and without tantalum were processed into 0.5-in.-thick plate and tested for tensile and Charpy impact properties. Tensile data were generated in four different conditions for each alloy: quenched and quenched and tempered (Q and Q&T) and normalized and normalized and tempered (N and N&T). Tensile tests were run from room temperature to 600°C. Tensile data were plotted as a function of test temperature and compared with the commercially available highest strength alloy in this class (T23). An example of such a plot for yield strength is shown in Figure 1. Observations from this figure and other figures showed: (1) the Fe-3Cr-3W(V) alloys of this study have very high yield and ultimate tensile strength in all four test conditions: Q, Q&T, N, and N&T; and (2) as compared to the commercial alloy T23, the Fe-3Cr-3W(V) alloys have nearly twice the yield strength across the entire test temperature range of room temperature to 600°C. The Charpy impact data for one of the two alloys tested in Figure 2 show that the alloy has exceptional impact properties in the quenched condition, which improves significantly by tempering. Data from Figure 2 also suggest that for many applications, the impact properties without the tempering heat treatment will meet the design toughness criteria. The welding of the plates from the Fe-3Cr-3W(V) alloys also showed good toughness properties without postweld heat treatment. These properties have led Nooter Consulting Services to develop many potential applications for the Fe-3Cr-3W(V) alloys.

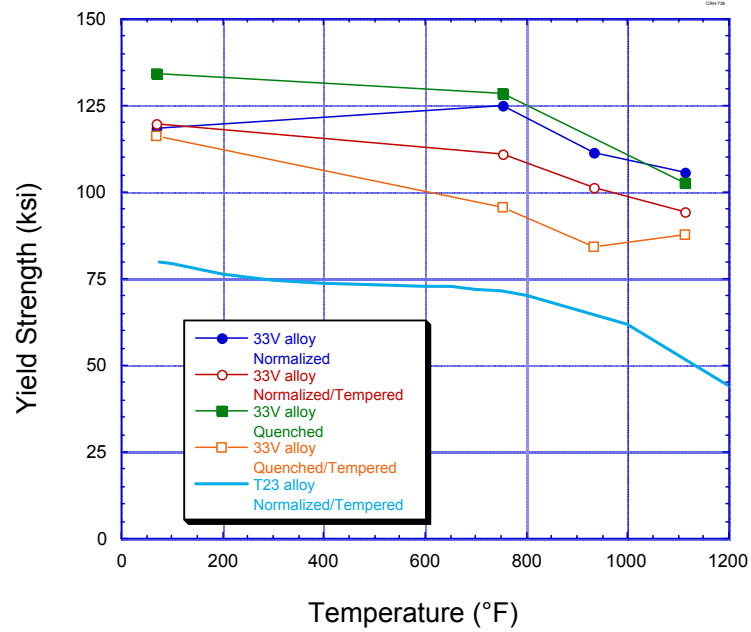


Fig. 1. Comparison of yield strength for Fe-3Cr-3W(V) alloy in quenched, quenched and tempered, normalized, and normalized and tempered conditions with the data for alloy T23.

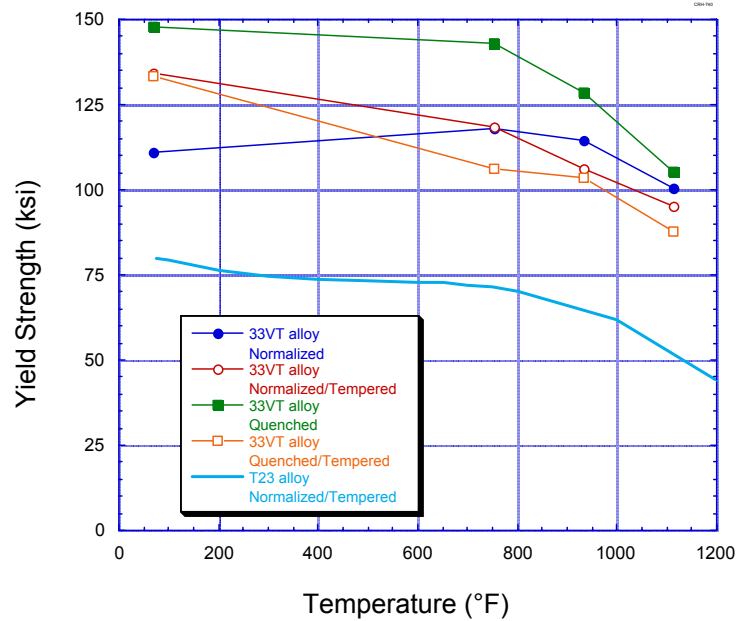


Fig. 2. Comparison of Charpy impact properties for Fe-3Cr-3W(V) alloy in quenched and quenched and tempered conditions.

**Reports/Publications/Awards:**

R. L. Klueh, V. K. Sikka, R. W. Swindeman, M. L. Santella, P. J. Maziasz, and M. H. Jawad, "Fabrication, Heat Treating Microstructure, and Tensile Testing of a High Strength 3Cr-3W-V(Ta) Alloy Plate," MPLUS report, January 2001.



**MPLUS No.:** MC-01-030

**Title:** Improving the Surface Finishing of Extruded 6262 Alloy Billet

**User Organization:** Alcoa Engineered Products  
Spanish Fork, UT 84660

**User Contact:** D. Mark Shelley, 801-798-8730  
[mark.shelley@alcoa.com](mailto:mark.shelley@alcoa.com)



Mark Shelley from  
Alcoa Engineered Products

**ORNL R&D Staff:** Qingyou Han, 865-574-4352  
[hanq@ornl.gov](mailto:hanq@ornl.gov)

**Relevance to OIT:** Aluminum

**Objective:** One issue during the extrusion of 6262 alloy billet is that material builds up at the die and bearing surfaces, leading to poor surface quality of the extruded billet. Such build-up can lead to scratches and decreased productivity. The purpose of this MPLUS project was to investigate the reasons for material build-up at the die surfaces in order to possibly increase the efficiency of the process. The relationship between phase fraction, size, and distribution of the soft phases in the billet will be determined.

**Results:** The microstructure of the specimens taken from the extruded billets was characterized. Contrary to speculations that the alloy contains “soft” phases such as Pb-Bi eutectics, a large number of hard  $Mg_3Bi_2$  particles were found in the specimen. No Pb-Bi eutectic phases were found. These hard intermetallic  $Mg_3Bi_2$  particles are likely to blemish the surface of the extruded aluminum.

Figure 1 shows the typical microstructure of an as polished specimen. It comprises of a dark colored particle phase and the gray matrix of 6061 aluminum alloy. On the surface perpendicular to the extrusion direction, the particles are spherical and their sizes are non-uniform. Most of the particles are small but there are also a few particles larger than 10  $\mu m$ .

The Energy Dispersive X-ray Spectroscopy (EDXS) analysis, shown in Figure 2, revealed that the particles in the extruded specimens were mainly composed of bismuth and magnesium, rather than lead and bismuth that are supposed to form low melting point (“soft”) Pb-Bi eutectic particles for the improved machinability. The magnesium and bismuth concentrations in the particles are 51.56 and 43.79 at. %, respectively. Lead concentration in the particles accounts for only 0.49 at. %. This is quite a surprise since lead and bismuth are specially added in the alloy in order to form lead-bismuth eutectics that melt at 125.5°C. The lead content in the binary lead-bismuth eutectic should be around about 55 at. %. Thus, the particles in the extruded specimens are not lead-bismuth eutectics at all.

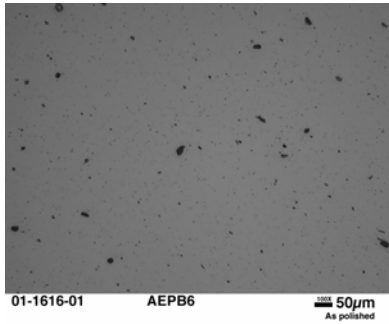


Fig. 1. The microstructure of an extruded specimen.

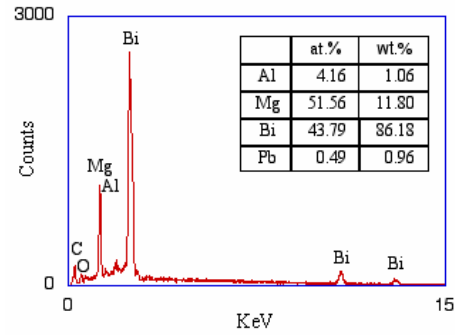


Fig. 2. An EDXS analysis of composition of particles.

The phase diagram of magnesium and bismuth is illustrated in Figure 3.  $Mg_3Bi_2$  is the only phase that exists in the alloy system apart from the magnesium and bismuth phases. The content of bismuth in  $Mg_3Bi_2$  is around 40 at. %, which is very close to the concentration of bismuth in the particles of the extruded specimens. This suggests that the particles shown in Figure 1 are  $Mg_3Bi_2$  particles rather than the lead-bismuth eutectic particles. Figure 3 also shows that the melting point of the  $Mg_3Bi_2$  phase is 821°C (1510°F), much higher than the melting point of the aluminum alloys. Thus, the formation of  $Mg_3Bi_2$  is most likely related to the diminished extruded surface quality, since the  $Mg_3Bi_2$  is a hard intermetallic phase with a high melting temperature. If these particles are trapped at the die bearing surface during extrusion of the 6262 alloy, they are able to blemish the surfaces of the extruded aluminum products.

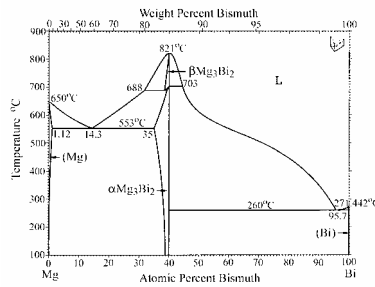


Fig. 3. The Mg-Bi phase diagram.

A comparison of the microstructure of a good surface quality specimen with that of the blemished specimens was carried out using image analysis. Over seven thousand particles in each sample were characterized. The particle size distributions in those three samples are very similar for the small particles. Over 95% (number percent) of the particles are smaller than 5  $\mu m$ . Difference exists for large particles in these two kinds of specimens. The specimen with good surface finish contains less and smaller large particles than those of blemished surface.



The maximum particle size in each field under optical microscope was measured. The maximum particle size is defined as the largest particle size in each field of  $500 \times 700 \mu\text{m}$ . The fields were randomly chosen and the results are shown in Figure 4. The maximum particle size in sample with a good surface finish was in the range between 10 and  $20 \mu\text{m}$ , whereas that of the sample with a poor surface finish was in the range between 10 to  $33 \mu\text{m}$ . The particle size in the samples with a poor surface finish can be as large as two times of that in the sample with a good surface finish.

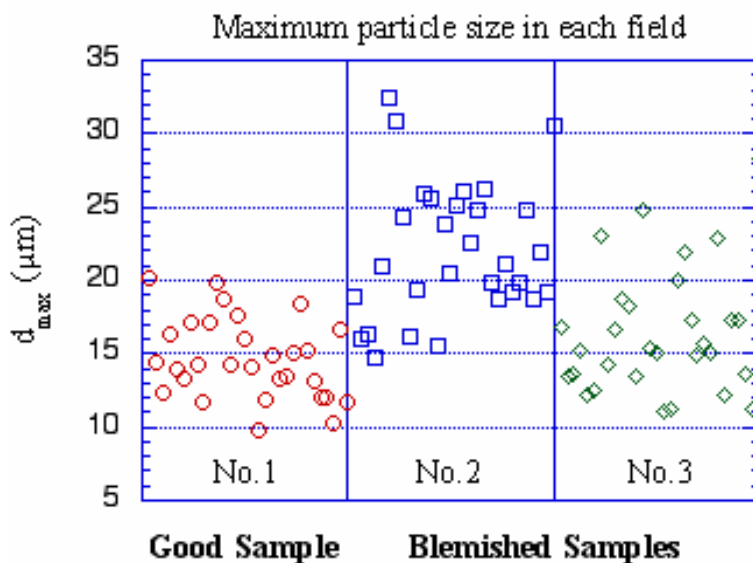


Fig. 4. The maximum particle sizes in the specimens. The large particles in the blemished specimens are much larger than those in the good specimen.

**Conclusions:** The extruded aluminum 6262 alloy contains a large number of hard  $\text{Mg}_3\text{Bi}_2$  particles rather than the soft eutectic Pb-Bi particles. The surface finish of the extruded products is related to the size and amount of the  $\text{Mg}_3\text{Bi}_2$  particles. Specimen with good surface finish contains less and smaller  $\text{Mg}_3\text{Bi}_2$  particles than those with a poor surface finish. These results can now be used to determine process improvements.

#### **Reports/Publications/Awards:**

Q. Han, S. Viswanathan, and M. Shelley, "Improving the Surface Finish of Extruded 6262 Alloy Billet," MPLUS report, July 2001.



**MPLUS No.:** MC-01-031

**Title:** Energy Savings during the Extrusion of 6061 Alloy

**User Organization:** Alcoa Engineered Products  
Spanish Fork, UT 84660

**User Contact:** D. Mark Shelley, 801-798-8730  
[mark.shelley@alcoa.com](mailto:mark.shelley@alcoa.com)



Mark Shelley from  
Alcoa Engineered Products

**ORNL R&D Staff:** Qingyou Han, 865-574-4352  
[hanq@ornl.gov](mailto:hanq@ornl.gov)

**Relevance to OIT:** Aluminum, Heat Treating

**Objective:** Currently, Aluminum 6061 billet is extruded at 941°F and fan cooled in AEP. It may be possible to optimize the process in terms of extrusion temperature and cooling rate for increased energy savings. The purpose of this MPLUS project was to investigate effect of cooling rate on the microstructure and the mechanical properties of aluminum billets of different thickness. Heat transfer during cooling of the extruded billet was determined. The microstructure of the billet was characterized and the hardness of the specimens was measured.

**Results:** Thermocouples were placed in the center and surface of the specimens and the cooling curves of the specimen under three cooling conditions (air cooling, fan cooling, and water quenching) were measured. Figures 1 and 2 show the cooling curves. Fan cooling cooled the specimen two times faster than air cooling.

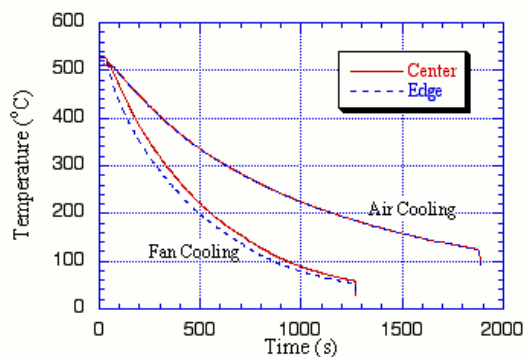


Fig. 1. Cooling curves for aluminum specimens under air cooling and fan cooling conditions.

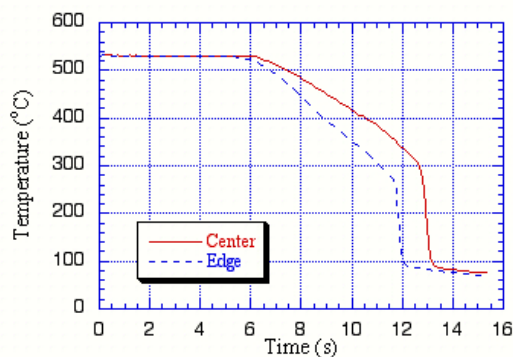


Fig. 2. Cooling curves of the water quenched specimens.

The hardness of the specimens is shown in Figures 3 and 4. The water quenched specimens were hardest. The fan-cooled specimens were harder than those cooled in air but the difference in hardness is not that large.

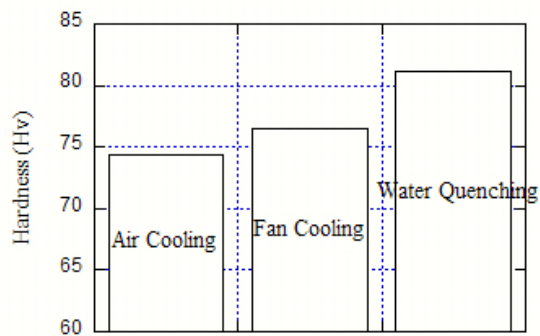


Fig. 3. The hardness of the 0.25-in. specimens.

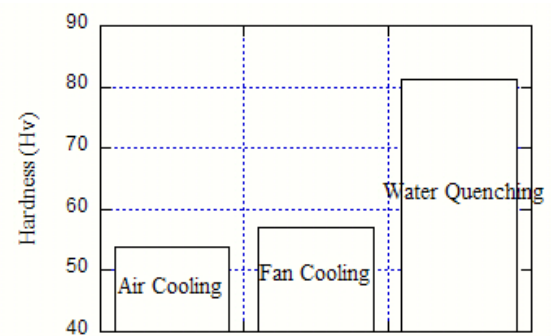


Fig. 4. The hardness of the 1-in. specimens.

The scanning electron microscope (SEM) images of the microstructure of the specimens cooled at various cooling rates are shown in Figures 5 through 7. There was not much difference between the specimens cooled in air than those cooled using a fan.

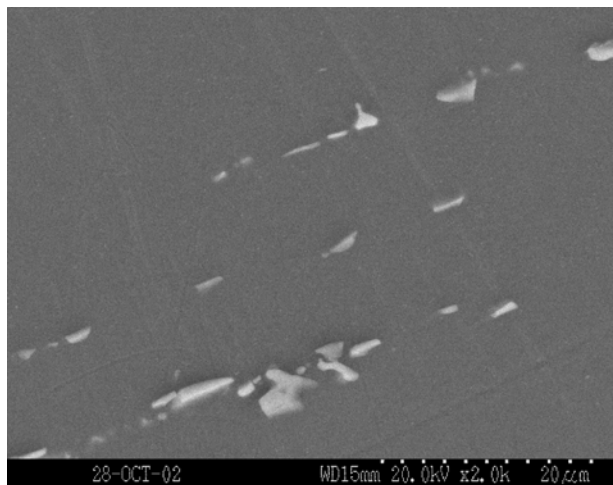


Fig. 5. Air cooling.

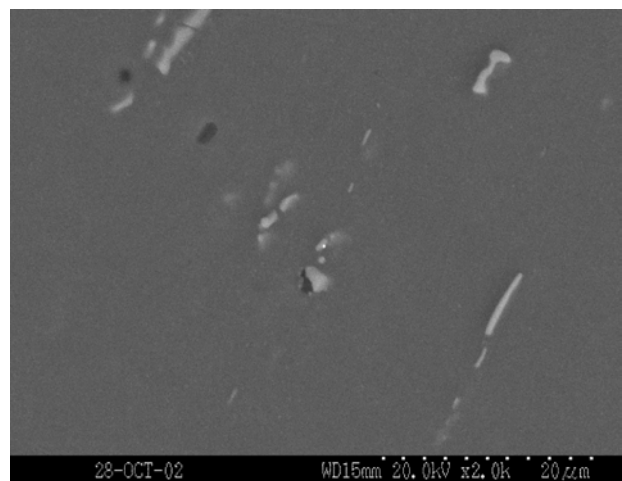


Fig. 6. Fan cooling.

These results indicate that fans cooling the aluminum extrusions may not necessary, leading to energy efficiency improvements.



Fig. 7. Nano-sized particles.

Another interesting result is that, at high magnifications, the air cooling and fan cooling specimens contained nano-sized particles. The effect of these particles on the mechanical properties is not known and may deserve further research.

**Reports/Publications/Awards:**

Qingyou Han and Mark Shelley, "Energy Savings during the Extrusion of 6061 Alloy," MPLUS report, October 2002.



**MPLUS No.:** MC-01-034

**Title:** Simulation of Sulfur Segregation in Steels

**User Organization:** Caterpillar Inc.  
Peoria, IL 61656-1875

**User Contact:** K. C. Hsieh, 309-578-6056  
[Hsieh\\_K\\_Cynthia@cat.com](mailto:Hsieh_K_Cynthia@cat.com)

**ORNL R&D Staff:** John M. Vitek, 865-574-5061  
[vitekjm@ornl.gov](mailto:vitekjm@ornl.gov)

**Relevance to OIT:** Mining, Steel, Heat Treating



Cynthia Hsieh from Caterpillar Inc.

**Objective:** Materials modeling may lead to valuable insight into the factors that influence the extent of sulfur diffusion and metastable phase formation, thus providing guidance for how to consistently produce ultra tough air-melted steels. The goal of this project was to: (1) simulate the diffusion of elemental sulfur to boundaries in steels under non-equilibrium conditions and the precipitation kinetics of various types of sulfides, (2) examine the effects of heat treatment time, temperature, and alloy compositions on sulfur segregation, and (3) investigate the interactions between sulfur and other alloying elements such as carbon, and the consequences of these interactions with regard to sulfur segregation.

**Results:** Preliminary calculations using computational thermodynamics were carried out to determine if sulfur segregation and metastable behavior could be explained. These efforts gave insufficient insight. No significant variation due to austenitizing temperature was found. These results, and the transient nature of the experimental results, suggested that the embrittlement was related to a kinetic phenomenon. Therefore, a kinetic diffusion analysis was undertaken.

A finite difference model that describes the simultaneous diffusion of sulfur and manganese to an inclusion interface was developed. It was assumed that the inclusion interface acted as a sink in that as sulfur and manganese diffused to the interface, MnS was formed. The model considered the distribution of sulfur in the vicinity of the interface, and how the sulfur concentration varied with time. Without precise information on the equilibrium concentrations of sulfur and manganese at the inclusion interface, and the diffusion coefficients of sulfur and manganese in the particular steel under investigation, the model was used in a qualitative manner to try to reproduce the experimental SAM results. In particular, it was used to see if the transient effects as a function of heat treatment condition could be explained.

The finite difference model considered the simultaneous diffusion of sulfur and manganese to the inclusion interface. The difference in diffusion rates for sulfur and manganese was critical in producing transient effects. The calculations were carried

out for a range of different relative diffusion rates. It was found that many of the experimental results could be duplicated with the model. For example, the effects of changing austenitization temperatures and times could be reproduced. The model showed that after relatively short austenitization times, the sulfur concentration near the inclusion interface was a minimum, corresponding to minimum embrittlement, and that with longer heat treatment times, the sulfur concentration increased once again, indicating the embrittlement would be worse. This behavior is identical to what was found experimentally. This effect was a consequence of the fact that initially, the sulfur near the interface combined with available manganese to form MnS and to reduce the residual sulfur level. However, after this initial decrease, the faster sulfur diffusion of sulfur leads to a re-accumulation of sulfur near the interface. Slower Mn diffusion was the rate-limiting step for the formation of additional MnS. A sample curve of the sulfur concentration at the interface as a function of time is shown in Figure 1. Since the actual diffusion coefficients were not well known, the actual “times” and “temperatures” of the calculation are not significant but rather the model should be used to predict trends.

The finite difference model provided valuable insight into the factors that may influence the extent of sulfur diffusion and metastable phase formation, thus providing guidance for how to consistently produce ultra-tough air-melted steels.

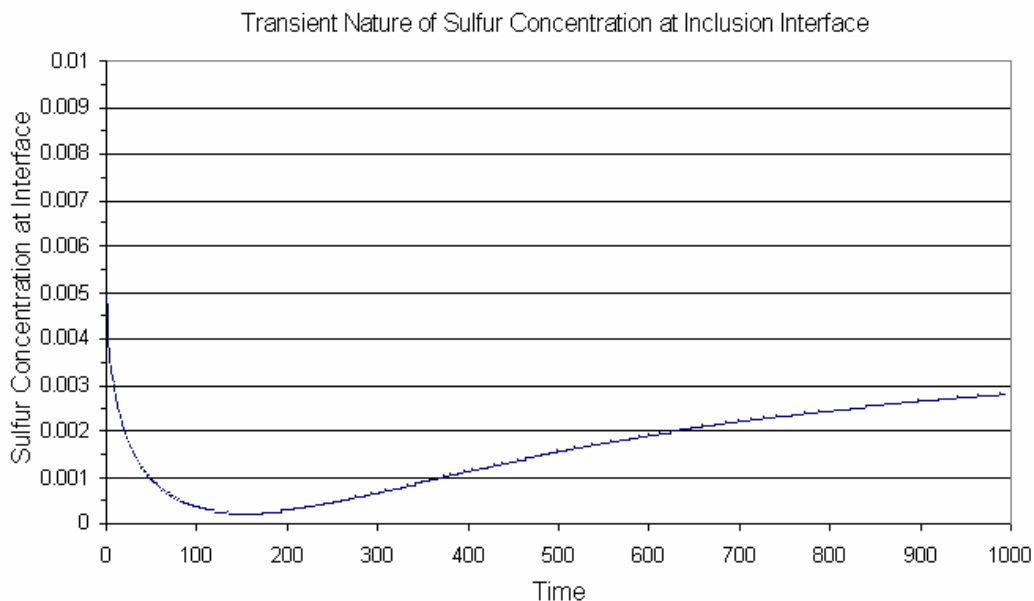


Fig.1: Calculated variation of sulfur concentration at an inclusion interface as a function of heat treatment time.

### Reports/Publications/Awards:

J. M. Vitek and K. C. Hsieh, “Simulation of Sulfur Segregation in Steels,” MPLUS report, April 2002.



**MPLUS No.:** MC-01-036

**Title:** Development of Seal Coatings for Ceramic Refractories for Molten Aluminum

**User Organization:** Pyrotek  
Trenton, TN 378382

**User Contact:** Russell P. Hale, 731-855-7712  
Rushal@pyrotek-inc.com

**ORNL R&D Staff:** A. J. Moorhead, 865-574-4667  
[moorheadaj@ornl.gov](mailto:moorheadaj@ornl.gov)  
J. O. Kiggans Jr., 865-574-8863  
[kiggansjojr@ornl.gov](mailto:kiggansjojr@ornl.gov)  
C. A. Blue, 865-574-4351  
[blueca@ornl.gov](mailto:blueca@ornl.gov)  
R. D. Ott, 865-574-5172  
[ottr@ornl.gov](mailto:ottr@ornl.gov)



Russell Hale from Pyrotek

**Relevance to OIT:** Metalcasting, Aluminum

**Objective:** The objective of this MPLUS project was to evaluate the feasibility of improved refractory components for use in aluminum casting. Specifically, it was hoped to evaluate low-cost approaches for sealing the surface porosity in slip cast molten aluminum feed pipes. Slurries of fine particles of similar compositions were formulated to the existing refractories and examined methods for applying these coatings to the slip castings before firing. Preliminary work was done using test coupons and the most promising were applied to full-sized tubes for testing in an actual aluminum caster.

**Results:** Infrared heating of Pyrotek samples was conducted in the infrared test facility at ORNL. Since large nozzles were not required for these early coating and infrared treatment trials, one of the nozzles was cut with a diamond cut-off saw into dozens of test sections (Figure 1). Various coatings were applied to the Pyrotek parts to judge whether they could be used as seal coats. Both coated and non-coated parts were heated at several infrared power settings. Following heat treatments, a control and infrared-heated uncoated samples were sectioned to produce sizes suitable for scanning electron microscope (SEM) analysis.

Figure 2 shows both coated and non-coated parts that were heated by infrared. A continuous melted surface was observed on the non-coated parts. The YAG coating did not melt evenly with this initial trial, but this novel melt appeared to be very promising, since the material is very refractory and melts at high temperatures.



Fig. 1. Photographs of as-received transfer tube and slices that were cut and ground flat from this tube.

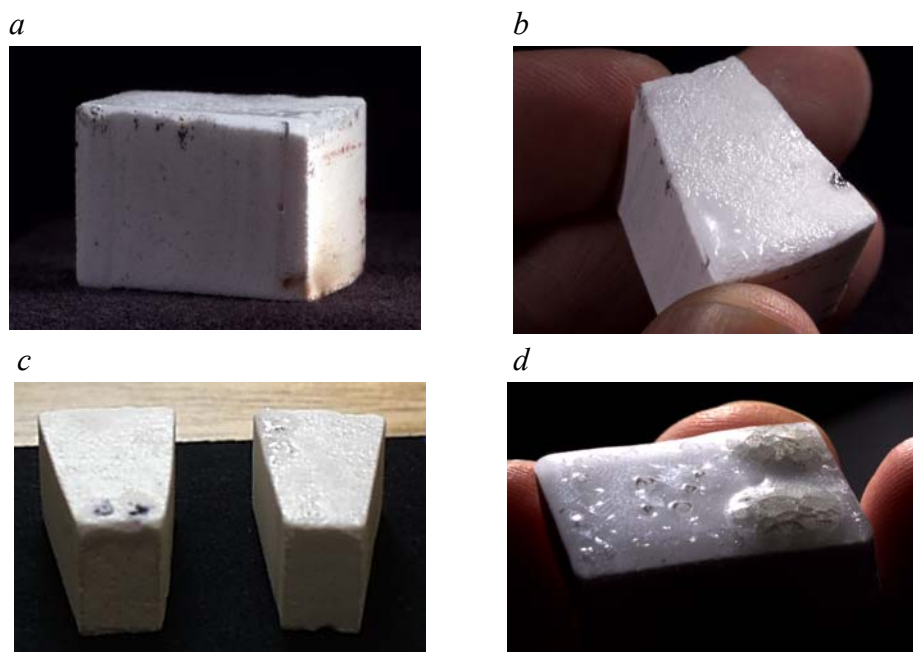


Fig. 2. Photographs of infrared Set 1: (a) and (b) as-received infrared-heated part, (c) parts coated with colloidal silica and infrared heated (left), and (d) YAG-coated part and infrared heated.

Figure 3 shows a scanning electron microscopy (SEM) photograph of the non-coated infrared-treated nozzle part. The high-magnification photo shows that the layer was very uniform and relatively thin. X-ray analysis (data not shown) showed that the melted surface was amorphous silica.

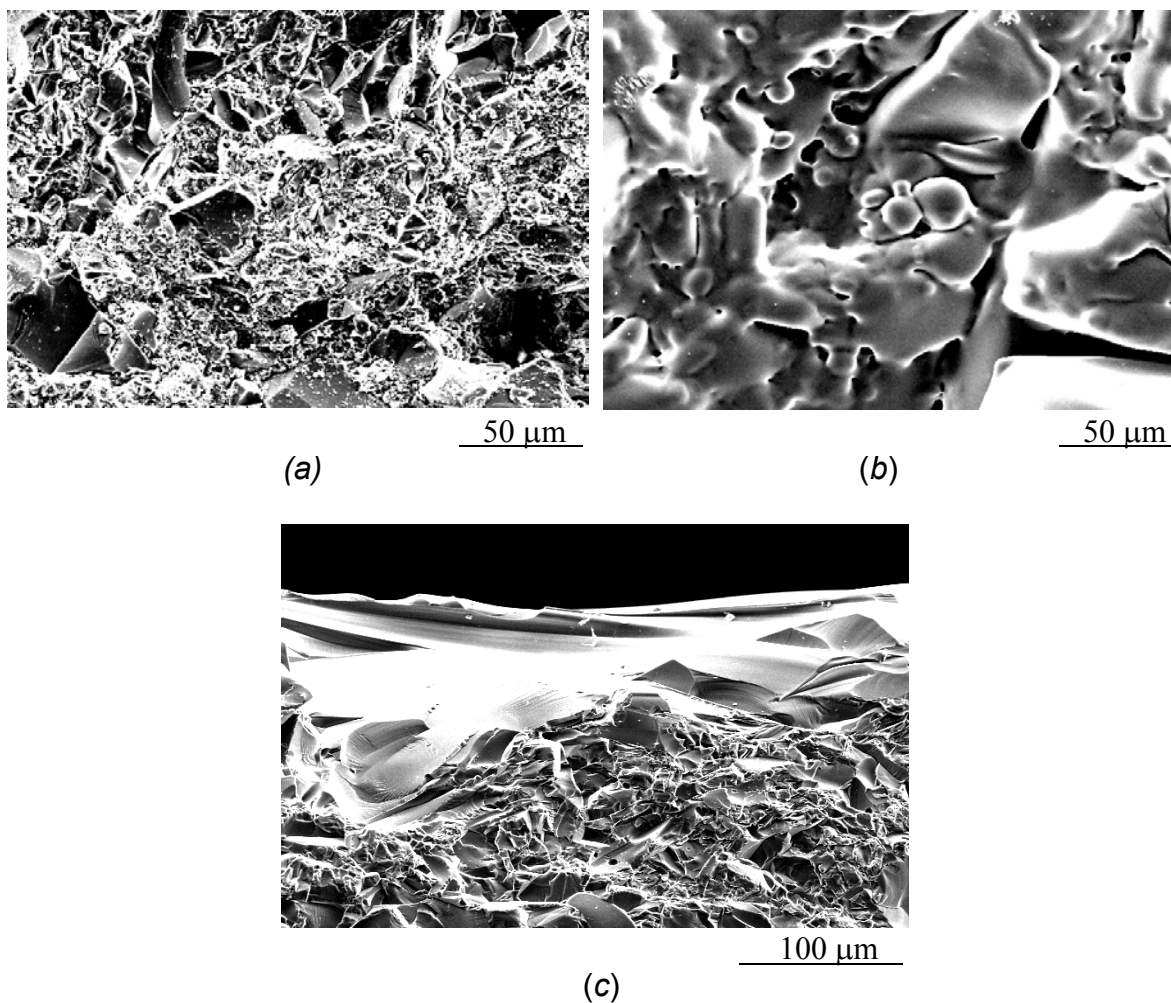


Fig. 3. Scanning electron microscopy images of: (a) top view of untreated Pyrotek material, (b) top view of infrared-heated Pyrotek material, and (c) side view of infrared-treated Pyrotek material.

#### **Reports/Publications/Awards:**

A. J. Moorhead, F. C. Montgomery, J. O. Kiggans Jr., D. C. Harper, C. Walls, and J. L. Dulberg, "Development of Seal Coatings for Ceramic Refractories for Molten Aluminum," MPLUS report, 2001.



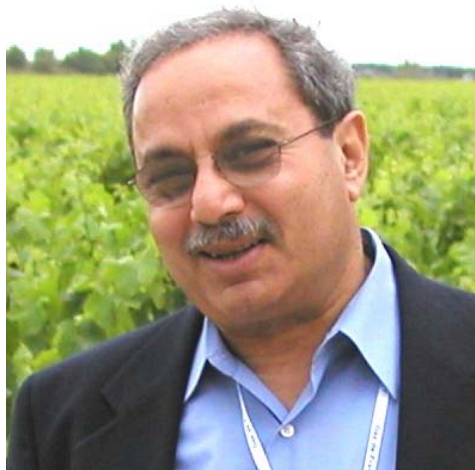
**MPLUS No.:** MC-01-037

**Title:** Thermochemical Optimization of Float Glass Composition

**User Organization:** Visteon Glass Systems  
Allen Park, MI 48101

**User Contact:** Edward Boulos, 313-755-1539  
[eboulos@visteon.com](mailto:eboulos@visteon.com)

**ORNL R&D Staff:** T. M. Besmann, 865-574-6852  
[besmanntm@ornl.gov](mailto:besmanntm@ornl.gov)



Edward Boulos from  
Visteon Glass Systems

**Relevance to OIT:** Glass

**Objective:** The objective of this MPLUS project was to optimize the float glass composition. Visteon Glass Systems uses 0.5 wt %  $\text{Al}_2\text{O}_3$  for the purpose of keeping the primary phase in the B-Wilstonite and avoiding the formation of tridymite and silica devitrification. Their objective was to remove/optimize or minimize the  $\text{Al}_2\text{O}_3$  in order to reduce cost and energy use by optimizing the  $\text{SiO}_2/\text{MgO}/\text{CaO}$  ratios in the composition. The critical properties were liquidus temperature, primary phases, viscosity, and chemical durability. Another objective was to optimize the float compositions by using other oxides that improve the properties mentioned above including cost and energy.

**Results:** The results to date are preliminary and further work is ongoing. The extended effort was required because existing models, including that developed at ORNL, do not have the precision required to answer the questions raised by Visteon. This is because of the very small changes in composition and the resulting modest changes in melting temperatures. This has caused us to request that Visteon wait until the ORNL has been further developed/refined, which should occur later this calendar year. The second action was to have several compositions more carefully explored using experimental means. The Pacific Northwest National Laboratory has therefore performed liquidus measurements on a series of compositions of glass. These are of interest to Visteon as well as providing a baseline for the comparison with the ORNL computation.

Despite the issue of having sufficient precision in the current glass model, ORNL has investigated how the glass system responds to compositional changes using the available model. It was used to investigate the effect on liquidus temperature of:

- $\text{Al}_2\text{O}_3$ : 0.1 and 0.45 wt %
- $\text{CaO}$ : +/- 0.5 wt %
- $\text{MgO}$ : +/- 0.5 wt %
- $\text{Na}_2\text{O}$ : +/- 0.5 wt %

Figures 1 and 2 below show some examples of the results illustrating trends in behavior.

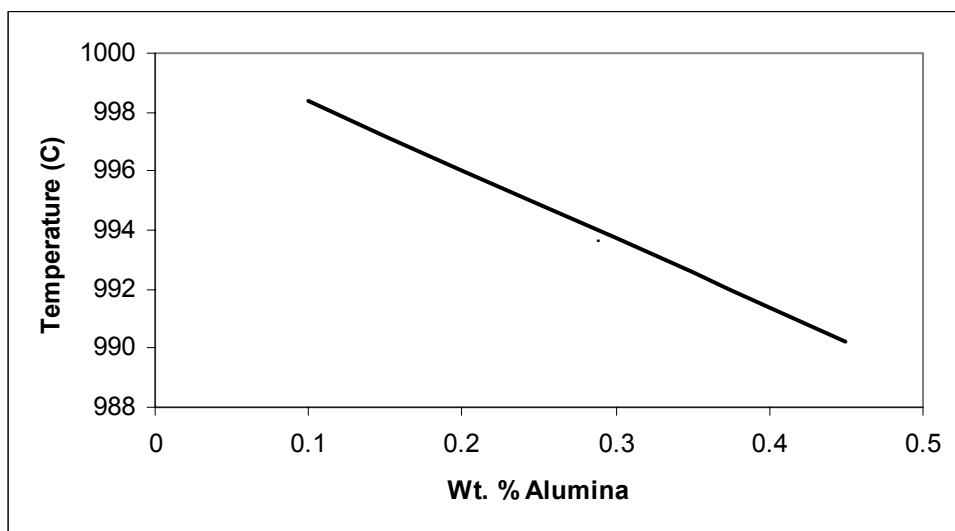


Fig. 1. A 0.35 wt % change in alumina content changes liquidus by  $\sim 10^{\circ}\text{C}$ .

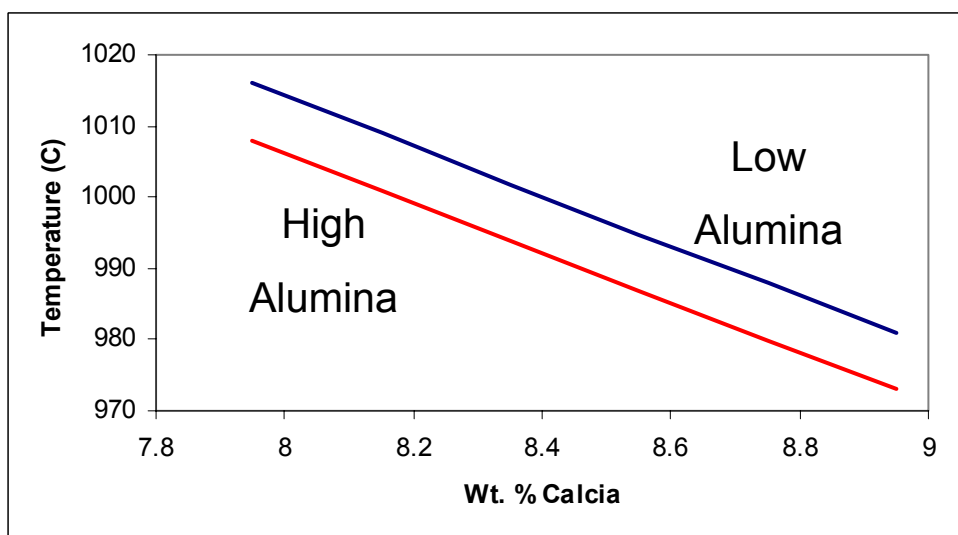


Fig. 2. Increasing calcia also reduces liquidus temperature, with 1% causing a  $35^{\circ}\text{C}$  change.

#### Reports/Publications/Awards:

T. M. Besmann and E. N. Boulos, "Thermochemical Optimization of Float Glass Composition," MPLUS report, February 2002.

**MPLUS No.:** MC-01-038

**Title:** Reactive-Gas Inert Anode Concept

**User Organization:** MMPaCT, Inc.  
Oak Ridge, TN 37830

**User Contact:** H. Wayne Hayden, 865-483-5740  
[hwhayden@cs.com](mailto:hwhayden@cs.com)

**ORNL R&D Staff:** R. A. Lowden, 865-576-2769  
[lowdenra@ornl.gov](mailto:lowdenra@ornl.gov)  
J. J. Henry, 865-574-4559  
[henryjjr@ornl.gov](mailto:henryjjr@ornl.gov)

**Relevance to OIT:** Aluminum



Wayne Hayden from MMPaCT, Inc.

**Objective:** A novel concept for the fabrication of an inert anode for use in an aluminum reduction cell was hypothesized. The anode utilized hydrogen or a hydrocarbon gas and a porous carbon structure to replace the carbonaceous materials currently employed in the application. Instead of the carbon from the anode being consumed during the reaction to produce aluminum and carbon dioxide, the gas would react with the alumina to form aluminum metal and water or water mixed with CO<sub>2</sub>. A small cell was built to test the concept. Cell characteristics and product gas composition were examined to evaluate the function of the cell and viability of the concept.

**Results:** Two each of the two types of electrodes were fabricated: a hollow graphite and an alumina sheath with a carbon foam insert. The newly machined foam shed flakes during gas formation on the first run only. As a result each electrode was cleaned by bubbling gas through the porous insert while immersed in acetone until the shedding stopped. The anode was then dried for 24 h and heated to 1000°C in argon prior to use in an experiment. A series of experiments were planned the details of which are noted in Table 1.

The first test was successfully completed [Figure 1(a) and (b)] and aluminum was produced (Figure 1(c)). A cryolite mixture of 90% Na<sub>3</sub>AlF<sub>6</sub> + 6% AlF<sub>3</sub> + 4% Al<sub>2</sub>O<sub>3</sub> was used for the initial experiments and the cell was operated at 4 to 6 V and 1 A/cm<sup>2</sup>, at a temperature of 960°C. The cell was tested using a solid graphite anode to gather baseline information. Inert gas was used to purge the system and the voltage and current density variations were recorded. The cryolite adhered to the surface of the anode; therefore, an accurate determination of weight loss could not be made even after destructive characterization of the anode. Additional experiments are planned using improved equipment.



Table 1. Experimental Plan for Inert Anode Using Graphite Foam

Anode Design	Temperature (°C)	Cryolite Composition	Reactive Gas	Purpose
Solid graphite	960	90% $\text{Na}_3\text{AlF}_6$ + 6% $\text{AlF}_3$ + 4% $\text{Al}_2\text{O}_3$	None	Verify cell operation
Hollow graphite with foam insert	960	90% $\text{Na}_3\text{AlF}_6$ + 6% $\text{AlF}_3$ + 4% $\text{Al}_2\text{O}_3$	None	Verify cell operation with foam insert
Hollow graphite with foam insert	960	90% $\text{Na}_3\text{AlF}_6$ + 6% $\text{AlF}_3$ + 4% $\text{Al}_2\text{O}_3$	Methane	Test foam with methane as reactive gas
Hollow alumina with foam insert	960	90% $\text{Na}_3\text{AlF}_6$ + 6% $\text{AlF}_3$ + 4% $\text{Al}_2\text{O}_3$	None	Verify cell operation
Hollow graphite with foam insert	960	90% $\text{Na}_3\text{AlF}_6$ + 6% $\text{AlF}_3$ + 4% $\text{Al}_2\text{O}_3$	Methane	Test foam with methane as reactive gas + inert shell

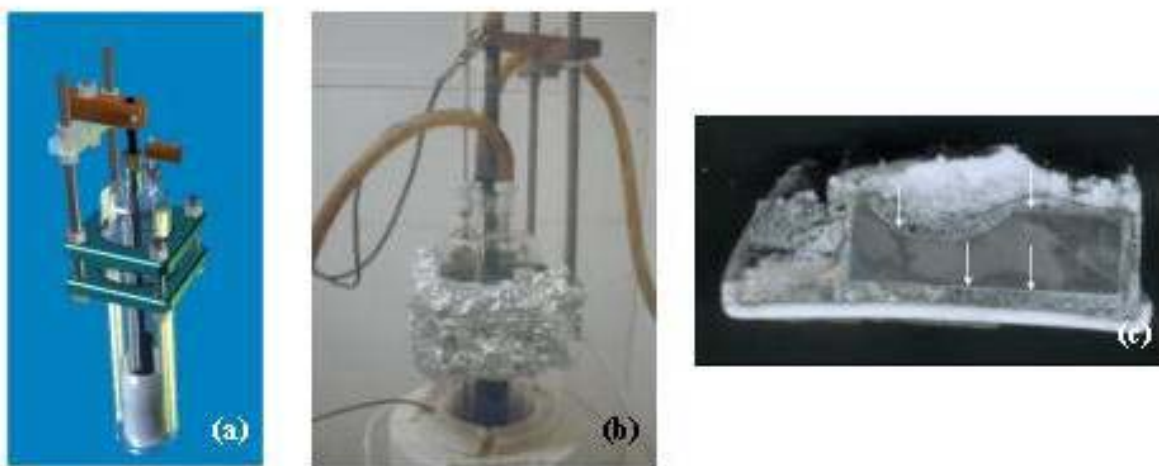


Fig. 1. (a) Test cell concept, (b) cell in operation, and (c) results of first run with aluminum noted by arrows.

#### Reports/Publications/Awards:

John Henry and Wayne Hayden, "Reactive-Gas Inert Anode," Interim MPLUS report, February 2002.



## LIST OF PROJECTS

---

### MPLUS Proposal List

Proposal No.	Organization	Proposal Title	Org. PI	ORNL PI	Relevance
MC-01-001	Vista Engineering Inc. Birmingham, AL	Stress Analysis in Thin Surface Layers	R. Thompson (205) 222-7419	B. Radhakrishnan (865) 241-3861	Chemical
MC-01-003	Caterpillar Inc. Peoria, IL	Development of Infrared Thermal Processing Techniques for Improving the Wear and Corrosion Resistance of Coatings	M. Brad Beardsley (309) 578-8514	Gail M. Ludtka (865) 575-4652	Mining Heat Treating
MC-01-004	Ispat Inland, Inc. East Chicago, IN	The Effect of Thermal Process Parameters on the Phase Transformation Behavior in Fully Austenitized, Medium-Carbon Alloy Steel	Gopal R. Nadkarni (219) 399-5661	Gerard M. Ludtka (865) 574-5098	Steel Heat Treating
MC-01-005	Babcock & Wilcox Barberton, OH	Recovery Boiler Wall Tube Temperature Measurements	John Kulig (330) 860-6438	Gorti Sarma (865) 574-5147 Jim Keiser (865) 574-4453	Forest Products Process Heating
MC-01-006	Babcock & Wilcox Barberton, OH	Analyses of Weld Overlay Tubes	Joan Barna (330) 860-6766	Gorti Sarma (865) 574-5147 Jim Keiser (865) 574-4453	Forest Products Welding
MC-01-007	GE Aircraft Engines Cincinnati, OH	Investigation of Oxidation of Super-alloys at High Pressures and Temperatures	Ben Nagaraj (513) 786-2287	P. F. Tortorelli (865) 574-5119	Combined Heat and Power
MC-01-009	Eagle Racing Loudon, TN	Evaluation of Filler Metals for Improved Elevated Temperature Strength of Aluminum Welds	M. R. Hedgecock (865) 408-1000	Jim King (865) 574-4807	Welding Metalcasting Aluminum
MC-01-010	Deformation Control Technology Cleveland, OH	Pyrowear 53: Dilatometry to Determine Phase Transformation Kinetics	Blake L. Ferguson (440) 234-8477	Gerald M. Ludtka (865) 574-5098	Heat Treating Forging Steel Mining
MC-01-011	Cummins Engine Co. Columbus, IN	Dilatometric Study of Phase Transformations and Resultant Phase Fractions in Forged 1550 Steel for Comparison to and Definition of the Microstructures of Induction-Hardened Parts	Roger D. England (812) 377-7573	Gerard M. Ludtka (865) 574-5098	Heat Treating Forging Steel

### MPLUS Proposal List (Continued)

Proposal No.	Organization	Proposal Title	Org. PI	ORNL PI	Relevance
MC-01-012	Logan Aluminum Russellville, KY	Detection of Fabrication Defects and Oxidation in Aluminum Castings	John Zeh (270) 755-6502	Qingyou Han (865) 574-4352	Aluminum Metalcasting
MC-01-013	Ohio State University Columbus, OH	Characterization of Heat-Treating Processes in Modified 383 Die Cast Aluminum	S. Raman (614) 688-3117	Gerard M. Ludtka (865) 574-5098	Metalcasting Aluminum
MC-01-014	Engineering Mechanics Corporation of Columbus (Emc <sup>2</sup> ) Columbus, OH	Hardenability of Next-Generation High-Strength Steels for Oil/ Natural Gas Transportation Pipelines	Zhili Feng (614) 459-3200	Suresh Babu (865) 574-4806	Steel Chemical Petrochemical
MC-01-015	Mead Central Research Chillicothe, OH	Statistical Analysis of Time-Series Data on Temperature and Resistivity Collected from Recovery Boiler Floor Tube Membranes	James D. Willis (740) 772-3748	Jim Keiser (865) 574-4453	Forest Products
MC-01-017	Thixomat Ann Arbor, MI	Preparation of Spherical Balls (1 to 2 mm diam) of a Magnesium Alloy for Improving Process Efficiency of Thixomolding®	D. M. Walukas (734) 995-5550 ext. 234	Vinod Sikka (865) 574-5112	Metalcasting
MC-01-019	Smith International, Inc. Houston, TX	Feasibility Study for Hot Extrusion of High Toughness Cemented Carbide Composites	Zak Fang (281) 233-5869	Vinod Sikka (865) 574-5112	Mining Petrochemical Powder Metallurgy
MC-01-020	Weirton Steel Corporation Weirton, WV	Select Alloys, Conduct In-Plant Tests, and Characterize Test Coupons of Candidate Hood Materials	H. M. Snyder (304) 797-4999	Vinod Sikka (865) 574-5112	Steel Welding Process Heating
MC-01-021	Haynes International Inc. Kokomo, IN	The Effect of Boron and Zirconium on the Resistance of HAYNES® 214™ Alloy to Strain Age Cracking	Mark D. Rowe (765) 456-6228	Suresh Babu (865) 574-4806	Chemical Combined Heat and Power
MC-01-022	Weyerhaeuser Company Federal Way, WA	Detection of Plant Cell Dimensions in Loblolly Pine using Micro-CAT Scan Techniques	N. C. Wheeler (360) 330-1738	M. J. Paulus (865) 241-4802	Forest Products
MC-01-023	Caterpillar Inc. Peoria, IL	Determination of True Stress-Strain Curves of Steels at Elevated Temperatures	Zhishang Yang (309) 578-2761	Suresh Babu (865) 574-4806	Mining Steel Welding

### MPLUS Proposal List (Continued)

Proposal No.	Organization	Proposal Title	Org. PI	ORNL PI	Relevance
MC-01-024	Native American Technologies Company Golden, CO	Forming of Thick Section Material using the Vortek Water Stabilized Plasma Lamp	Jerry Jones (303) 279-7942 ext. 20	Gail M. Ludtka (865) 576-4652	Steel Heat Treating
MC-01-025	University of South Carolina Columbia, SC	Residual Stress Determination in Friction Stir Welded 2024-T3 Aluminum	M. A. Sutton (803) 777-7158	Cam Hubbard (865) 574-4472	Welding Aluminum
MC-01-026	Ford Motor Company Dearborn, MI	Soldering/Brazing for Automotive Aluminum Panels using Arc Lamp as a Heating Method	Tsung-Yu Pan (313) 322-6845	Mike Santella (865) 574-4805	Welding Aluminum
MC-01-028	Alcoa Engineered Products Spanish Fork, UT	Rapid Infrared Preheating of Extrusion Die	Mark Shelley (801) 798-8730	Craig A. Blue (865) 574-4351	Aluminum Forging
MC-01-029	Nooter Consulting Services St. Louis, MO	Fabrication, Heat-Treating Microstructures, and Tensile Testing of a High-strength 3Cr-3W-V(Ta) Alloy Plate	Maan H. Jawad (314) 421-7339	Vinod Sikka (865) 574-5112	Chemical Steel Petrochemical Process Heating
MC-01-030	Alcoa Engineered Products Spanish Fork, UT	Improving the Surface Finishing of Extruded 6262 Alloy Billet	Mark Shelley (801) 798-8730	Qingyou Han (865) 574-4352	Aluminum
MC-01-031	Alcoa Engineered Products Spanish Fork, UT	Energy Savings during the Extrusion of 6061 Alloy	Mark Shelley (801) 798-8730	Qingyou Han (865) 574-4352	Aluminum Heat Treating
MC-01-034	Caterpillar Inc. Peoria, IL	Simulation of Sulfur Segregation in Steels	Cynthia Hsieh (309) 578-6056	John M. Vitek (865) 574-5061	Mining Steel Heat Treating
MC-01-036	Pyrotek Trenton, TN	Development of Seal Coatings for Ceramic Refractories for Molten Aluminum	Russell P. Hale (731) 855-7712	Jim Kiggans, Jr. (865) 574-8863	Metalcasting Aluminum
MC-01-037	Visteon Glass Systems Allen Park, MI	Thermochemical Optimization of Float Glass Composition	Edward Boulos (313) 755-1539	Ted Besmann (865) 574-6852	Glass
MC-01-038	MMPaCT, Inc. Oak Ridge, TN	Reactive-Gas Inert Anode Concept	Wayne Hayden (865) 483-5740	Rick Lowden (865) 576-2769	Aluminum



## **STAFF CONTACTS AND GENERAL INFORMATION**

---

Staff contacts and general information are provided below for additional information:

**Program:**

Dr. Peter Angelini, Program Manager  
Oak Ridge National Laboratory  
One Bethel Valley Rd.  
Oak Ridge, TN 37831-6065  
Phone: (865) 574-4565, Fax: (865) 576-4963, Email: [angelinip@ornl.gov](mailto:angelinip@ornl.gov)

**General information and submittals:**

Ms. Millie Atchley  
MPLUS Administrative Specialist  
Metals Processing Laboratory User (MPLUS) Facility  
Oak Ridge National Laboratory  
One Bethel Valley Rd.  
Oak Ridge, TN 37831-6083  
(865) 574-4358, Fax: (865) 574-4357, Email: [atchleyml@ornl.gov](mailto:atchleyml@ornl.gov)

**User Center Leaders:**

**Processing:**

Dr. Vinod Sikka, (865) 574-5112, Email: [sikkavk@ornl.gov](mailto:sikkavk@ornl.gov),

**Joining:**

Dr. Stan David, (865)574-4804, Email: [davidsa1@ornl.gov](mailto:davidsa1@ornl.gov),

**Characterization:**

Corrosion: Dr. Peter Tortorelli, (865) 574-5199, Email: [tortorellipf@ornl.gov](mailto:tortorellipf@ornl.gov)

Mechanical: Dr. Edgar Lara-Curzio, (865) 574-1749, Email: [laracurzioe@ornl.gov](mailto:laracurzioe@ornl.gov)

**Materials/Processing Modeling:**

Dr. B. Radhakrishnan, Phone: (865) 241-3861, Email: [radhakrishnan@ornl.gov](mailto:radhakrishnan@ornl.gov)

Additional information and proposal applications are available at URL:

<http://www.ms.ornl.gov/emfacility/mplus/mplus.htm>



## **ACKNOWLEDGEMENT**

---

Research sponsored by the U.S. Department of Energy, Office of Energy Efficiency and Renewable Energy, Industrial Technologies Program, Industrial Materials for the Future, and Aluminum Industry of the Future under contract DE-AC05-00OR22725 with UT-Battelle, LLC.

